Master's Thesis

A Coordinated Optimization Algorithm of Inter-RAT Handover Thresholds and Time-to-Trigger in Self-Organizing Networks

Liang Jiasheng

Department of Electrical and Information Technology,
Faculty of Engineering, LTH, Lund University, March 2014.

Master's Thesis

A Coordinated Optimization Algorithm of Inter-RAT Handover Thresholds and Time-to-Trigger in Self-Organizing Networks

By

Liang Jiasheng

Department of Electrical and Information Technology
Faculty of Engineering, LTH, Lund University
SE-221 00 Lund, Sweden

Abstract

The limited coverage of Long Term Evolution (LTE) system results in many inter-radio access technology (RAT) handovers from LTE to legacy second generation (2G) or third generation (3G) mobile system and vice versa. Trouble-free operation of inter-RAT handovers requires the optimization of the handover parameters of different RATs. Currently, the handover parameters are optimized manually and it requires human intervention and increases operational expenditures (OPEX). To reduce costs and achieve an improved network performance, a self-optimizing algorithm for the inter-RAT handover parameters is foreseen in upcoming Self-Organizing Networks (SON) standards. The parameters affecting the inter-RAT handovers are mainly signal strength (or quality) thresholds and a timer called Time-to-Trigger (TTT).

This thesis continues by further exploring the optimization of TTT using a coordinated approach with handover thresholds on the basis of the existing inter-RAT mobility robustness optimization (MRO) algorithm.

Evaluations are performed by different parameter coordination paradigms which present the best inter-RAT handover performance on various User Equipment (UE) speeds.

Acknowledgments

Firstly I would like to thank Nokia Siemens Networks (NSN) for offering me an opportunity to explore new research in my favour subject. I want to thank my great colleagues in NSN radio system for providing me an excellent working environment and their helpful attitude towards my work. Special thanks to Ahmad Awada, Bernhard Wegmann, Ingo Viering for their guidance to my research. And in particular, I would like to thank my colleagues Ömer Bulakci, Federica Vitiello, Dereje Kifle, Fasil Berhan for their encouraging comments and advice throughout my working period in NSN.

I further extend my thanks to my examiner of this thesis, Professor Ove Edfors at University of Lund.

Finally, I would like to thank my parents for their love throughout my everlasting studies, and for the thirst for knowledge they infected me with.

Munich, 2012
Anson Jiasheng Liang

Table of Contents

CHAPTER 1
Introduction

1.1 Self-Organizing Networks

During the last decade, telecommunication industry developed rapidly. The key mobile services have become more diverse ranging from voice calls, video streaming and internet web browsing. The developed 'Third Generation' (3G) mobile system and recently emerging Long Term Evolution (LTE) technology have played a significant role in sustaining mass data communication. The deployment of these series of network upgrades leads to a new layout of cells, which in general adds additional layers over the existing macro layers. As a result, Radio Access Technology (RAT) infrastructure has drifted from single RAT to Multi-RAT with complex layout of cells and heterogeneous network topology.

To improve the Quality of Services (QoS), the multi-layer networks needs to be properly configured and maintained which in turn increase the Operational Expense (OPEX) of the mobile operators. Unfortunately, those costs will not be compensated by additional revenue due to the decreasing average revenue per user (by pricing schemes like e.g. flat rate, induced through fierce competition in the market) [1]. In addition, the associated OPEX are also significant, as they comprise the costs of the specialized experts need for configuring manually the networks, and performing drive tests. Moreover, many kinds of risks cannot be neglected either, such as time-consuming execution, substantial delay in response of tuning, and potentially error-prone [2].

In order to reduce OPEX and eliminate the risks of manual operations, Self-Organizing Networks (SON) techniques are foreseen for LTE and they are recently developing rapidly as standardized work in 3rd Generation Partnership Project (3GPP).

1.2 Inter-RAT Mobility Robustness Optimization

The new LTE mobile system will overlay pre-existing mobile systems such as 'Second Generation' (2G) and 3G mobile systems in the first phase of deployment. As a result, the limited LTE coverage will yield many inter-RAT handovers from LTE to 2G/3G and vice versa.

Mobility Robustness Optimization (MRO) is applied to guarantee proper mobility for the users, that is, proper handovers between cells of the same, but also of a different RAT [1]. Currently, the handover parameters of all cells in a RAT are commonly configured during the network planning phase. Those cells which show later mobility problems during operation are optimized manually by Radio Network Optimization (RNO) specialists according to the analysis of system KPI statistic data and drive test log files. Therefore, expert knowledge becomes a vital factor for the success of the manually based optimization. Furthermore, time-consuming manual operation increases operator's OPEX as well as it is unable to timely adapt to the changing mobility conditions in each cell. From that perspective, a self optimizing algorithm for the inter-RAT handover parameters is required to provide a better user experience and reduce the costs.

MRO is an important use case of SON. Intra-RAT MRO for LTE mobile system has extensively investigated in papers [3], [4], [5], [6], [7]. An increasing number of extensive studies for inter-RAT MRO exist such as the investigation of inter-RAT handover parameters [8] and a general protocol for optimizing any kind of inter-RAT configuration parameters in [9]. Recently a SON-based algorithm for optimizing inter-RAT handover thresholds of LTE and 3G mobile systems was proposed in [10]. The proposed algorithm is run independently by each cell in both RAT where each cell updates its handover thresholds automatically based on the value of its KPIs. However, the latter algorithm optimizes only two handover thresholds corresponding to the serving cell and target cell of handover. There exist other parameters that impact the handover. Time-to-Trigger (TTT) which has been proposed in [11] is one of these parameters and refers to a time interval denoted by T_{T} which can delay or accelerate the execution of the handover [12]. Now how to utilize this additional degree of freedom jointly with handover thresholds becomes a new topic in SON-based optimization algorithm.

1.3 The Scope and Goal of the Thesis

Understanding the concept of SON and relevant 3GPP standards is essential to be able to probe the influenced entities and parameters which can be used to provide better the mobility KPI performance. The knowledge of measurement events triggering UE handed over and the inter-RAT handover procedure are equally important to know if the signal situation of a UE satisfies all the inter-RAT handover requirements. In the context of having TTT as an additional parameter for optimization, it is necessary to investigate the root cause of each inter-RAT mobility failure event which can be solved by optimizing the TTT value. After theoretical study, the thesis work focus on developing a complete solution for inter-RAT MRO which takes TTT optimization into account together with the existing optimization of the inter-RAT handover thresholds proposed in [10]. Thus the study of proposed SON-based algorithm for optimization of handover thresholds is a part of developing extensive MRO algorithm. Finally the impact on the performance will be investigated by applying different configuration paradigms and TTT step-adjustment strategies. The initial goal of this thesis is to develop a new joint optimization algorithm which mitigates more mobility failures upon the current MRO algorithm.

1.4 Structure of the Thesis

The contents of this thesis are divided into two parts which are literature study and algorithm development. The first part is as follows: Chapter 2 introduces measurement events in LTE and 3G and the inter-RAT handover procedure based on the measurement of UE. Chapter 3 presents the definition of inter-RAT mobility KPIs and an existing SON-based algorithm by running [10]handover threshold update in an automatic manner. The second part of the thesis consisting of Chapter 4 and 5 is the development and performance of a joint optimization algorithm. Chapter 4 focus on the root cause analysis against mobility failure due to misconfigured TTT and the joint optimization algorithm considering handover thresholds and TTT. Chapter 5 provides the comparison results of KPI performance between different algorithms and paradigms. Finally Chapter 6 summarizes the work in this thesis and makes suggestions for future work.

CHAPTER 2
Measurement Events and Handover Procedure

2.1 Measurements of the UE

To perform handovers, a User Equipment (UE) is required to measure the received signal or quality from the serving cell and all neighboring handover target cells. When the neighboring cells operate on a different carrier frequency compared to the current cell, the UE should carry out such measurement with measurement gaps [13]. The idea of measurement gaps is that the UE is able to switch to the target cell by switching the hardware oscillator in order to perform the signal quality measurement of a different frequency band during a small gap when there's no transmission and reception. The margin inside a measurement gap is needed for changing the reception frequency and configuring receiver to another RAT [14].

The UE measurements which are used in handover procedure are defined in 3GPP specifications in [15]. In LTE mobile system, the UE can measure either Reference Signal Receive Power (RSRP) or Reference Signal Receive Quality (RSRQ). The RSRP is defined for each cell as the linear average over the power distribution of the resource elements that carry cell-specific reference signals within the considered measurement frequency bandwidth [15]. Reference signals are allocated in resource units of 12 sub-carriers, resulting in 180 kHz allocation units called Physical Resource Block (PRB) [16].

Besides RSRP, RSRQ is also an important measurement, which gives an indication of the signal quality, especially when UE is moving near the cell border where interference is strong. The RSRQ is identical to the ratio of RSRP to the Received Signal Strength Indicator (RSSI) in the standard of Evolved Universal Terrestrial Radio Access (E-UTRA), shown as follows:.

$$RSRQ = \frac{N * RSRP}{RSSI} \tag{1}$$

where N is the number of PRB's inside the E-UTRA RSSI measurement bandwidth.

The E-UTRA RSSI comprises the linear average of total received power observed only in Orthogonal Frequency-Division Multiplexing (OFDM) symbols containing reference symbols by the UE from all sources [15]. In our case, RSSI is measured on 4 OFDM symbols with gross of 48 symbols in a single PRB distributed as follows: 8 reference symbols, 10 symbols from the Physical Downlink Control Channel (PDCCH) informing the UE about the resource allocation, and 30 symbols from Physical Downlink Shared Channel (PDSCH) with pure user data, as illustrated in Fig.1.

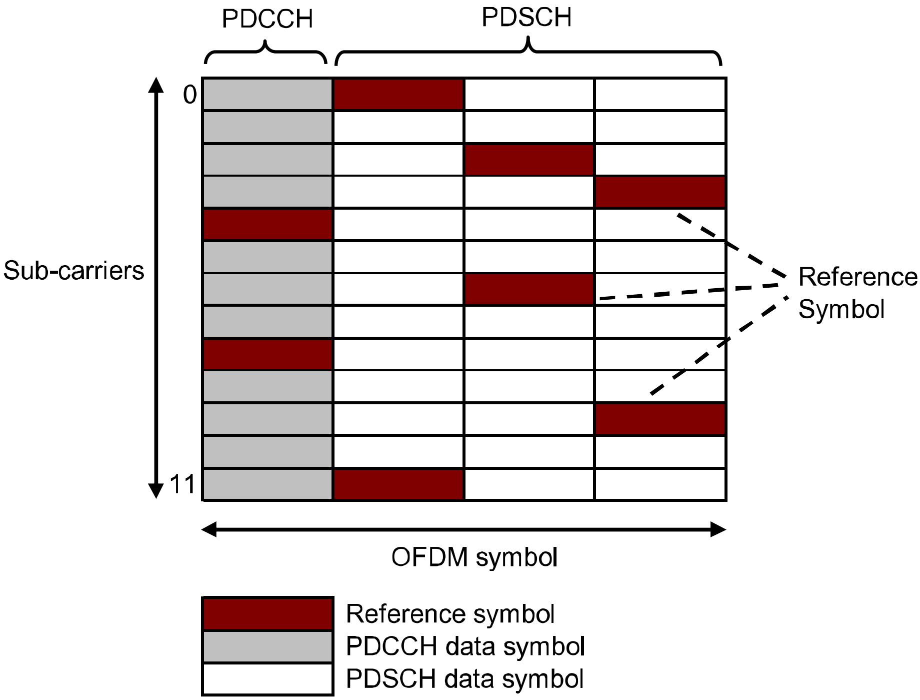

Fig. 1 Downlink resource blocks sharing structure for LTE

In Universal Mobile Telecommunication System (UMTS), Received Signal Code Power (RSCP) is comparable to the RSRP in LTE. The RSCP defines the received power on one code measured on the Primary Common Pilot Channel (CPICH) [17]. Similarly, CPICH Ec/No as the received energy per chip divided by power density in the band is comparable to RSRQ in LTE. CPICH Ec/No is identical to the ratio of CPICH RSCP to RSSI in the standard of UMTS Terrestrial Radio Access (UTRA), shown as follows:

$$Ec/No = \frac{RSCP}{RSSI} \tag{2}$$

2.2 Measurement Events B2 and 3A for Inter-RAT Handovers

Before an inter-RAT handover, the UE sends the report when a condition called the entering condition of a measurement event is fulfilled for a time interval T_{T}. In 3GPP standards, the serving cell configures the UE with a measurement event B2 [12] when the UE is handed over from a LTE cell to another cell of a different RAT. The entering condition of the measurement event B2 is fulfilled when the signal strength $S_{m,c}(t)$ of UE m connecting to a LTE serving cell c fails below a signal threshold S^{thr} in dBm and the signal strength $T_{m,c'}(t)$ of target cell c' in a different RAT is above another threshold T^{thr} in dBm, as depicted in Fig.2(a).

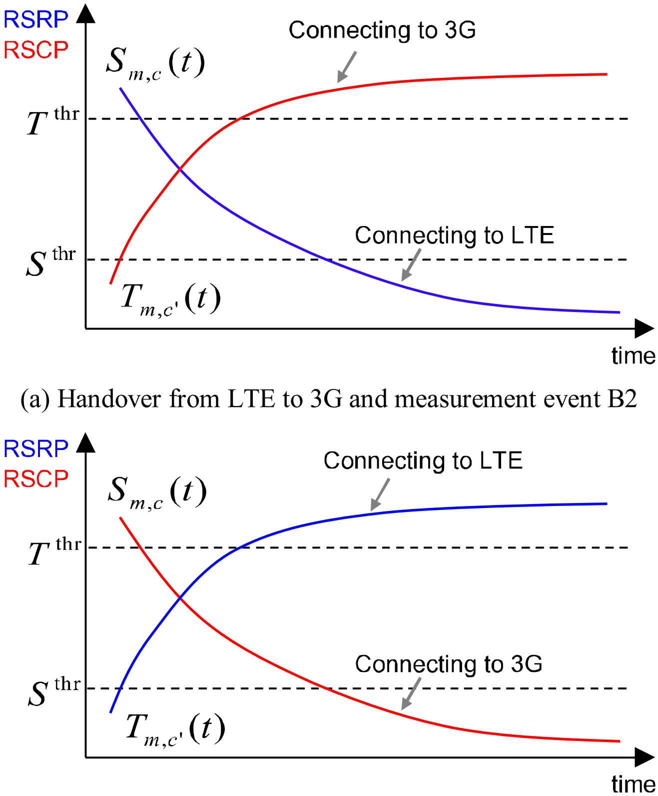

(b) Handover from 3G to LTE and measurement event 3A

Fig. 2 Examples of the entering condition of B2 and 3A measurement event

Vice versa, the measurement event is called 3A when the UE is handed over from 3G to another RAT [12]. The entering condition of the measurement event 3A is fulfilled when the signal strength $S_{m,c}(t)$ of UE m connecting to a 3G serving cell c fails below a signal threshold S^{thr} in dBm and the signal strength $T_{m,c'}(t)$ of target cell c' of another RAT is above another threshold T^{thr} in dBm, as depicted in Fig.2(b).

In our context, $S_{m,c}(t)$ and $T_{m,c'}(t)$ correspond either to RSRP or RSCP depending on the RAT of the measured cell. The thresholds of entering condition which are denoted by S^{thr} and T^{thr} are called inter-RAT handover thresholds.

2.3 The Inter-RAT Handover Procedure

Inter-RAT handover between LTE and 3G mobile system applies a UE-assisted handover algorithm. In the downlink, the serving cell in LTE or 3G network configures the UE. In the uplink, UE measure the signal strength or quality in a report for serving cell and inter-RAT neighboring handover target cells. The criterion for UE to send its measurement reports to the serving cell is either periodic or event-driven.

In case of event-driven reporting, the UE sends a measurement report to the serving cell c at time instant t_0 when the entering condition of measurement event is fulfilled for a time interval T_T as follows:

$$S_{m,c} < S^{\mathrm{thr}} \wedge \ T_{m,c'} > T^{\mathrm{thr}} \quad \text{for } t_0 < t < t_0 + T_{\mathrm{T}} \tag{3}$$

After receiving the measurement report, the serving cell prepares the handover of the UE by sending a handover request to the target cell in a different RAT. This handover preparation induces an additional delay of T_{HP}. Upon receiving an acknowledgement from the target cell, the UE is handed over to the target cell and the previously serving cell releases the resources allocated for that user.

2.4 Radio Link Failure in Inter-RAT Handover

Before the execution of a handover, the UE may drop during the handover procedure due to Radio Link Failure (RLF) when Signal-to-Interference and Noise Ratio (SINR) $SINR_{m,c}$ of the UE m connecting to serving cell c is continuously lower than a failure threshold Q_{fail} for a time interval of duration $T_{Q_{\text{fail}}}$ [8]. This model of RLF detection in LTE is the simplification of the RLF detection procedure defined in the 3GPP standard [18]. Thus, the handover of UE m from cell c to cell c' in another RAT at time instant t_{HO} is successfully executed when the following conditions are satisfied:

$$\begin{aligned} & S_{m,c} < S^{\text{thr}} \wedge T_{m,c'} > T^{\text{thr}} \quad \text{and} \quad SINR_{m,c} > Q_{\text{fail}} \\ & \qquad \text{for } t_{\text{HO}} - T_{\text{HP}} - T_{\text{T}} < t < t_{\text{HO}} - T_{\text{HP}} \end{aligned} \tag{4}$$

In order to reduce the inter-RAT handover problems caused by RLF, handover parameters are optimized properly at the lower cost such as the coverage loss of a RAT.

CHAPTER 3
Current SON-Based Algorithm for the Optimization of Inter-RAT Handover Thresholds

3.1 Introduction

The general idea of this algorithm is to optimize the two inter-RAT handover thresholds of S^{thr} and T^{thr} each in an automatic way using the value of predefined KPIs which captures the type of mobility failure events and the event numbers. This algorithm detects the root cause analysis of each inter-RAT mobility failure event and maps the value of KPIs into 4 new directives depending on the action required to be performed on each of the two handover thresholds, e.g., either increase or decrease. The magnitude of the change to be performed on each of the thresholds is determined by a feedback controller [19] and a gain scheduler [10], e.g., increase or decrease by a regular fixed step size or a smaller step size when oscillations in the values of KPIs occur. The mobility failure issues are reducing in each manipulated adjusting step of handover threshold, and eventually, it reaches a steady improved state of network performance.

3.2 Inter-RAT Mobility KPIs

The more details the KPIs are the better MRO solution is. Following the classification of the mobility failure event specified for intra-RAT scenario [11], two categories of KPIs have been extended in inter-RAT scenario [10]. The first one is RLF that is induced by strong interference or loss of coverage due to wrong handover execution time. The second one is called costly handovers which are successful handovers but inefficiently utilize radio resources.

RLFs are classified as Too Late Handover (TLH), Too Early Handover (TEH), and Handover to Wrong Cell (HWC).

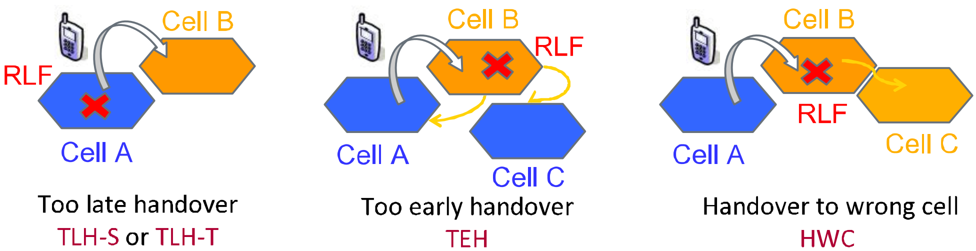

Fig. 3 RLFs consisting of TLH, TEH and HWC..

TLH: A UE losses connection before an inter-RAT handover is executed and reconnects to the previously serving cell. The reason for TLH is that the entering condition of measurement event has not been fulfilled duo to the misconfiguration of S^{thr} and T^{thr}. TLH-S and TLH-T has been adopted by 3GPP standard [20] to distinguish a TLH caused by the misconfiguration of the serving cell threshold S^{thr} and the target cell threshold T^{thr}, respectively.

TEH: A UE is successfully handed over from one RAT to another, but shortly after, the UE drops and reconnects to the previously serving cell or another cell of previous RAT. In addition, a special case is also considered as a TEH where an inter-RAT handover failure happens when the UE fails to access the target handover cell by using Random Access Channel (RACH) [13]. TEH is caused when T^{thr} is configured with a small value and the signal strength of the target cell is not strong.

HWC: A UE is successfully handed over from cell c to another cell c' of a different RAT, and shortly after, the UE drops and reconnects to cell c'' which is the same RAT of cell c'. Similar to TEH, the root cause of HWC is the misconfiguration of the target threshold T^{thr}, which should be set high enough to guarantee a strong target cell.

The second category of KPIs is costly handovers which are successful handovers. Though these handovers are less critical than radio link failures from user perspective, they are of significant importance for mobile operators as they require lots of network resources and generate signaling overhead between RATs. Ping-Pong (PP) and Unnecessary Handover (UH) are two classes of costly handovers.

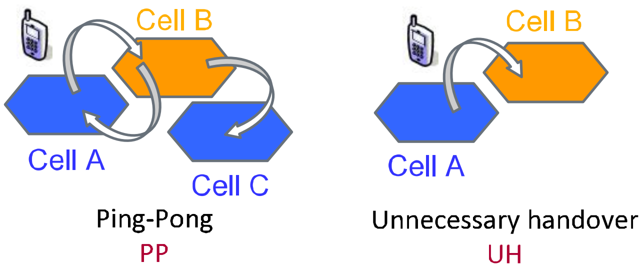

Fig. 4 Costly handovers consisting of PP and UH.

PP: A successful inter-RAT handover is executed, and shortly after, the UE is handed over back to a cell of the previous RAT occurs. Frequent ping-pong handovers increase the time of handover and thus the loading of the networks. The root cause of PPs is the high setting of S^{thr} or low setting of T^{thr}.

UH: Handovers from higher prior RAT (LTE) to lower prior RAT (3G) could be avoided. High number of UHs indicated that the coverage of the LTE is not fully exploited. As a result, users can not benefit from LTE from the perspective of mass data communication. UHs are caused by a high configuration on S^{thr}.

3.3 Description of the Entire Optimization Loop

In this section, we describe the two main components of the entire optimization loop of the handover thresholds which is depicted in Fig.5.

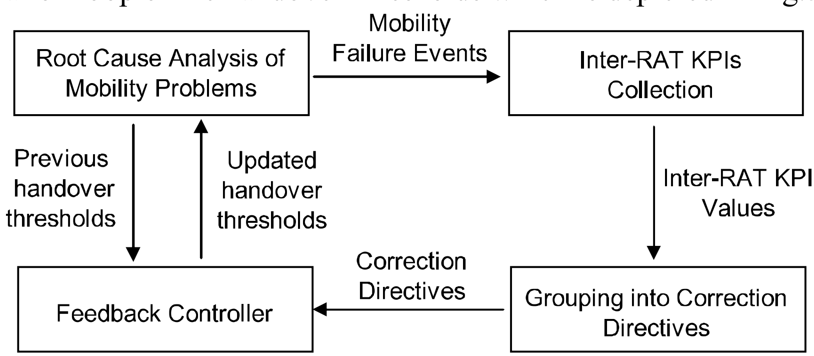

Fig. 5 The entire optimization loop for handover thresholds.

3.4.1 Root Cause Analysis and Collection of the Inter-RAT KPIs

A mobility failure event is collected by the cell of which the misconfiguration of its handover thresholds is responsible for that failure. The responsible cell collects the values of the inter-RAT KPIs in each KPI collection period k during a duration of T_{KPI}. The value of TLH-S, TLH-T, TEH, HWC, PPs and UHs collected by a cell in KPI period k are denoted by $N_k^{\mathrm{TLH-S}}$, $N_k^{\mathrm{TLH-T}}$, N_k^{TEH}, N_k^{HWC}, N_k^{PP} and N_k^{UH}, respectively.

3.4.2 Grouping the Values of the KPIs into Collection Directives

The collection of the KPI values is stopped at the end of each KPI period. The value of the mobility failure events collected in KPI period k are grouped into two pair of correction directives defined as follows: S_k^+ and S_k^- are defined as the number of mobility failure events which require an increase and decrease, respectively, in the value of serving handover thresholds S_c^{thr} in a KPI period k. Similarly, T_k^+ and T_k^- are the number of mobility failure events which require an increase and decrease, respectively, in the value of handover target thresholds $T_{c'}^{\mathrm{thr}}$ in a KPI period k. The values of inter-RAT KPI and their mapping to new correction directives are illustrated in Fig.6.

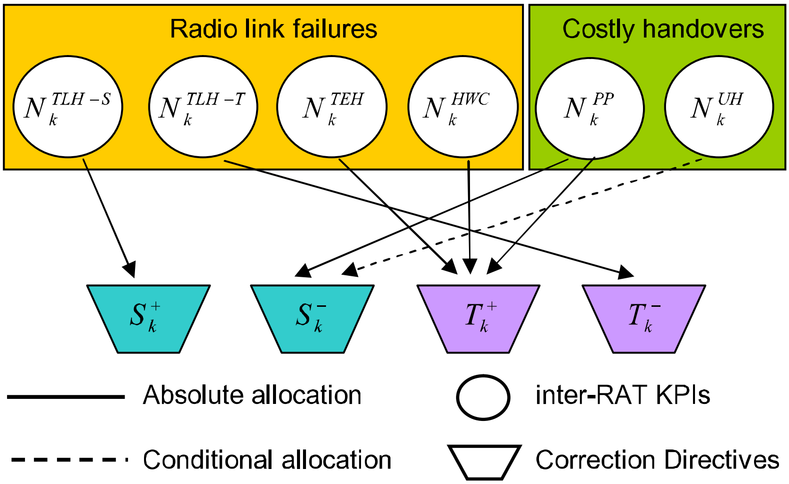

Fig. 6 Grouping the values of inter-RAT KPIs into new correction directives

It's worth noting that the value of UHs N_k^{UH} is exclusive for LTE. Moreover, mapping N_k^{UH} to S_k^- is valid only when TLHs does not exist.

3.4.3 Actions on the Handover Thresholds

The aforementioned four group values S_k^+, S_k^-, T_k^+ and T_k^- are utilized as input variables for the feedback controller in order to determine the updated values of the handover thresholds S_c^{thr} and $T_{c'}^{\mathrm{thr}}$. The feedback controller consists of a proportional control block and a gain scheduler as depicted in Fig.7. The proportional control block is designed to calculate the magnitude of a change that needs to be applied to each handover threshold value [10]. The magnitude of a change depends on the rate of the difference of the correction directives corresponding to a certain threshold, e.g., S_k^+ and S_k^-. The larger the rate, the larger the magnitude of a change is. In other words, the change of handover thresholds is proportional to the rate.

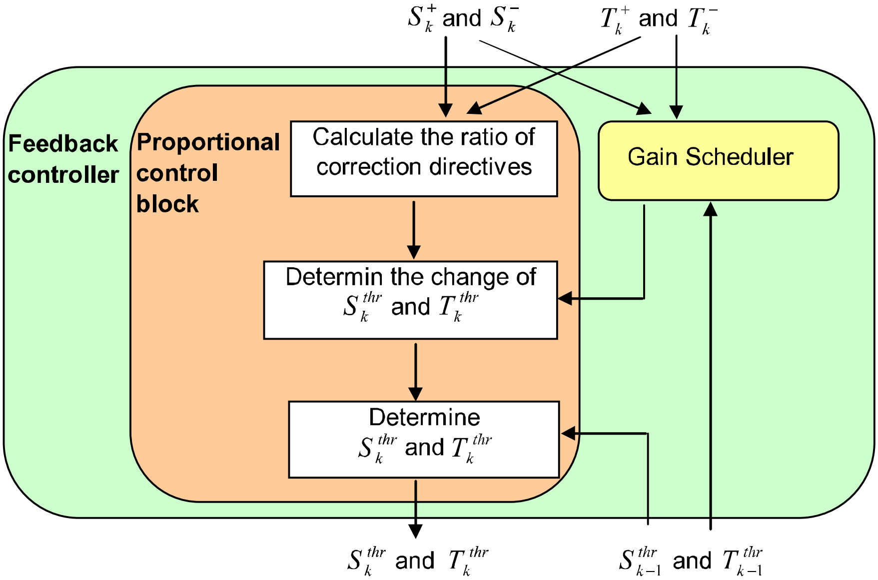

Fig. 7 The feedback controller consisting of a proportional control block and a gain scheduler

In some case, oscillation between the values of correction directives may occur. For example, a decrease on S_k^- may result in an increase in S_k^+ and vice versa. In this case, the mobility failure events of S_k^+ and S_k^- cannot be reduced simultaneously. To reduce these oscillations, a gain scheduler is used to alter the parameters of the proportional feedback controller so that the magnitude of change applied to the handover threshold reduces with each oscillation until a stable state is reached.

3.5 *Defects of the Current Approach*

TTT optimization is not considered in the current SON-based algorithm for the optimization of inter-RAT handover parameters. The algorithm assumes that a referenced TTT value, typically a small value, is configured during network planning phase to account for fast changing channel condition and take quick handover decisions. However, this low initial value of TTT reduces a large number of TLHs on the expense of an increasing number of TEHs or costly handover such as PPs and UHs. Moreover, the algorithm might not even converge if the TTT is configured by mistake to a very large value. Thus, the performance of the SON-based algorithm optimizing only the handover thresholds may vary depending on the initial configured value of TTT.

In addition, in some case the mobility failure events of S_k^+ and S_k^- cannot be reduced simultaneously. As a result, the oscillation occurs and stability is not achieved.

To address these two limitations, we propose a new SON-based algorithm which jointly optimizes the handover thresholds and TTT. As the optimization of TTT value has been proposed in [11], how to utilize this additional degree of freedom jointly with handover thresholds becomes a new topic in SON-based optimization algorithm. A performance gain from jointly optimization of handover thresholds and TTT will be investigated in our work.

CHAPTER 4
Joint Optimization of Handover Thresholds and TTT

4.1 *Introduction*

Some literatures such as [9] have presented a general MRO protocol for inter-RAT configuration parameters. A SON-based algorithm for a specific parameter of handover threshold was described in [10]. The algorithm optimizes only the handover thresholds assuming that the network-wide (NW) TTT is properly configured during network planning phase. Although a proposed method with simulative investigation in [21] presents a proper TTT selection for each specific UE speed, it only applies to intra-RAT handovers in LTE mobile system. Few papers have investigated the joint optimization of handover thresholds and TTT parameter for LTE and 3G mobile communication systems. However, in inter-RAT MRO case, there are some of the TLHs which can be exclusively adjusted by the handover thresholds [10], e.g., adjustment of TTT cannot help. Therefore, a joint optimization of TTT and handover thresholds is required to achieve a complete solution for inter-RAT MRO. For this purpose, we extend the existing SON-based algorithm for the optimization of handover thresholds, described in [10], by considering TTT as an additional degree of freedom to mitigate the mobility failure events and achieve additional gain in mobility performances.

4.2 *Description of the New SON-based Algorithm for Joint Optimization of Hanover Thresholds and TTT*

The entire joint optimization loop is illustrated in Fig.8. The root cause analysis of the new SON-based algorithm is more detailed than that discussed in section 3.2 for SON-based algorithm optimizing only the handover thresholds. This is needed to determine which cases of the KPIs can be exclusively adjusted by handover thresholds or TTT. After the root cause analysis, each type of mobility failure events are collected by different inter-RAT KPIs periodically. The classified inter-RAT KPIs are then mapped to handover thresholds or TTT correction directives as demand indicators which require a change in the corresponding handover parameters.

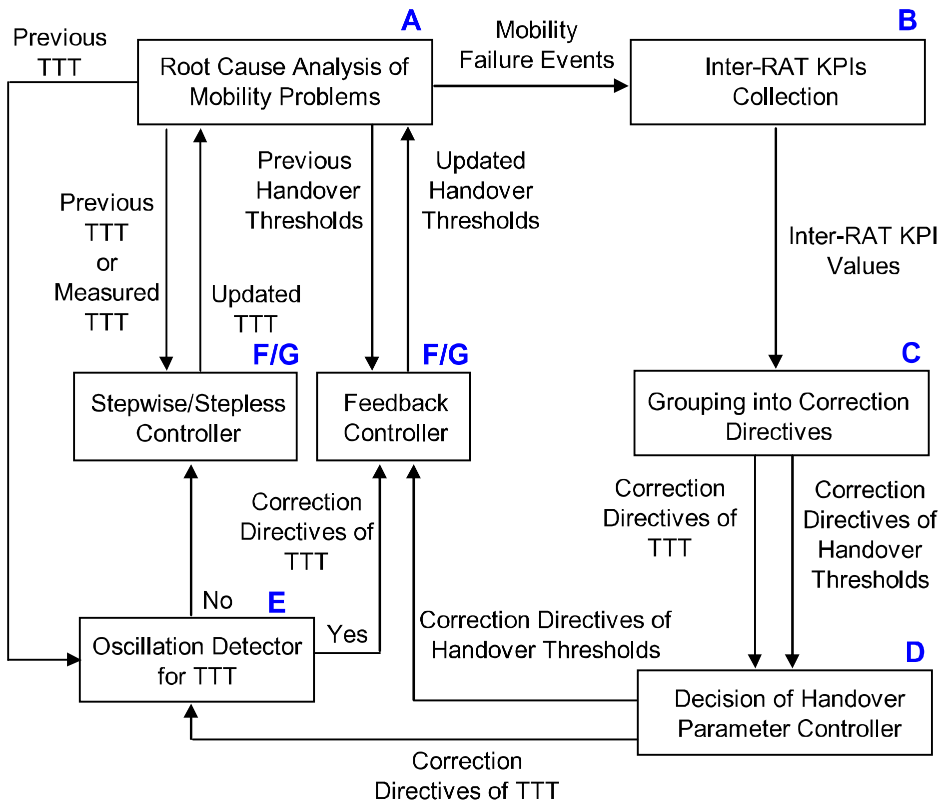

Fig. 8 The entire optimization loop of TTT and handover thresholds.

The action on handover threshold or TTT is determined by a decision of handover parameter controller and an oscillation detector for the value of TTT. The role of the decision of handover parameter controller is to determine whether the handover thresholds or TTT needs to be adjusted. If the handover thresholds need to be adjusted, their corresponding correction directives are passed to the feedback controller which determines the action required to be performed on the value of the handover thresholds as described in [10]. On the other hand, if TTT needs to be adjusted, its corresponding correction directives are passed to oscillation detector in order to check whether the value of TTT has converged or not. In case of convergence, the correction directives are mapped back to those of the handover thresholds and the feedback controller updates the handover thresholds taking into account all the values of KPIs. Otherwise, the correction directives of TTT are passed to the step controller which determines TTT by a fixed step size [12]. In Section 4.7, we further propose a new method which directly reaches the local optimal TTT value of the defined rang of TTT without the need to use a fixed step size for TTT.

4.3 *Root Cause Analysis*

In this section, we determine the case of each KPI which can be either exclusively mitigated by handover thresholds or TTT or both of them. A successful handover to a target cell in another RAT which is different from the previous serving cell is formed in accordance to two compulsory main conditions: fulfilled entering condition of measurement event and its fulfilled duration which exceeds a required time interval T_{T}. If one of the above conditions is not met, the inter-RAT mobility KPIs are partitioned off into two groups of KPIs, namely correction directives of handover thresholds and correction directives of TTT.

1) TLH

There are three TLH cases, denoted by A, B, and C, where the entering condition of measurement event is not fulfilled. For these cases, only the handover thresholds should be adjusted since the entering condition is not even fulfilled.

Case A: $T_{m,c'}(t)$ does not reach above $T_{c'}^{\mathrm{thr}}$. TLH is caused by the misconfiguration of handover threshold $T_{c'}^{thr}$ as depicted in Fig.9(a).

Case B: $S_{m,c}(t)$ does not reach below S_{c}^{thr}. TLH is caused by the misconfiguration of handover threshold S_{c}^{thr} as depicted in Fig.9(b).

Case C: None of the two thresholds are reached. TLH is caused by the misconfiguration of handover thresholds S_{c}^{thr} and $T_{c'}^{\mathrm{thr}}$ as depicted in Fig.9(c).

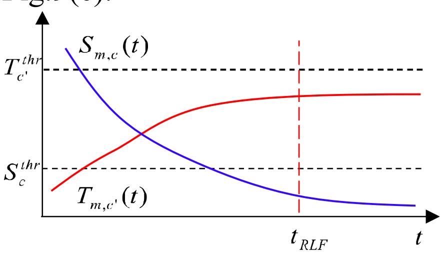

(a) Case A which is caused by the misconfiguration of handover thresholds.

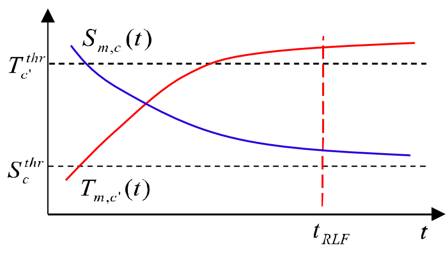

(b) Case B which is caused by the misconfiguration of handover thresholds.

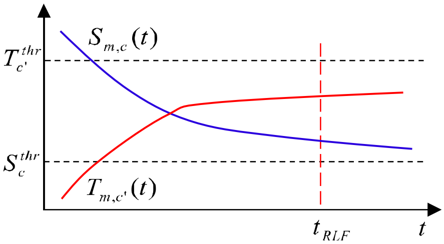

(c) Case C which is caused by the misconfiguration of handover thresholds.

Fig. 9 Three exclusive cases for TLH due to misconfigured handover thresholds.

In another four TLH cases denoted by case D, E, F and G as shown in Fig.10, the entering condition of measurement event is fulfilled. However, the RLF occurs before the execution of the handover. The three different cases D, F, and G can be fixed by either adjusting the handover thresholds or TTT. Whereas case E can be fixed only by adjusting TTT value. In what follows, the four cases are explained in details.

Case D: The RLF which occurred before the time interval of TTT is completed as depicted in Fig.10(a). This TLH can be resolved by either adjusting the serving threshold or shortening the value of TTT so that the handover to target cell c' can be completed before the UE suffers a RLF in serving cell c. To avoid this TLH, the TTT interval T_{T} and the handover preparation time interval T_{HP} should have elapsed between the two time instants t_{RLF} and t_0. Thus, the prerequisite condition for considering this case as possible TTT-TLH KPI is defined in (5).

$$T_{\mathrm{T}}^{\min} + T_{\mathrm{HP}} < t_{\mathrm{RLF}} - t_0, \quad \text{where } T_{\mathrm{T}}^{\min} = \min(I_{T_{\mathrm{T}}}) \tag{5}$$

where $T_{\mathrm{T}}^{\min}$ is the smallest value from the range of TTT value $I_{T_{\mathrm{T}}}$ in the specification defined by 3GPP [12].

Case E: The TLH shown in Fig.10(c) can be only resolved by shortening TTT value. This is because the entering condition of measurement event is always fulfilled and in turn the handover thresholds cannot have impact on making the handover earlier. Only if T_{T} value is shorten, the inter-RAT handover to target cell c' can be completed before the UE suffers a RLF in serving cell c as depicted in Fig.10(d). The preconditions for considering this case as a TTT-TLH KPI is as same as (5) of case D.

Case F: In this case of TLH, shown in Fig.10(e), the target signal has reached the target threshold for a short time before falling again. This TLH can be configured by either adjusting TTT or the handover thresholds. In the former case, the TTT interval T_{T} and handover preparation time interval T_{HP} should have elapsed between the time instant t_0 and t_{capture} which indicates the first time instant when $T_{m,c'}(t)$ fell below the target threshold $T_{c'}^{\mathrm{thr}}$. In this case, the handover to target cell c' would have been executed and a RLF at t_{RLF} might have been avoided as illustrated in Fig.10(f). The precondition for considering this case as TTT-TLH KPI is as follows:

$$T_{\mathrm{T}}^{\min} + T_{\mathrm{HP}} < t_{\mathrm{Capture}} - t_0 , \qquad (6)$$
$$\text{where } T_{\mathrm{T}}^{\min} = \min(I_{T_{\mathrm{T}}})$$

Case G: This case of TLH, illustrated in Fig.10(g), is similar to case F except that the serving signal fell below the serving threshold for a short time before increasing again. Again, if TTT interval T_{T} and handover preparation time interval T_{HP} have elapsed between t_0 and t_{capture}, the TLH would have been avoided as shown in Fig.10(h). The prerequisite condition for considering this case as TTT-TLH KPI is the same as condition (6) for case F.

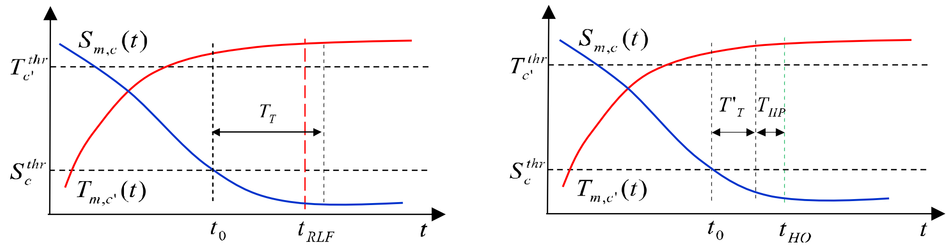

(a) Case D of TLH which can be fixed by either adjusting handover thresholds or TTT.

(b) The new value of TTT solving the TLH of case D.

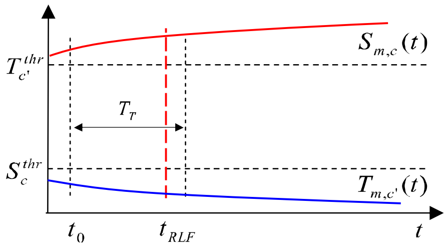

(c) Case E of TLH which can be fixed by either adjusting TTT.

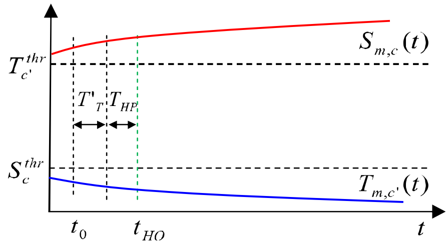

(d) The new value of TTT solving the TLH of case E.

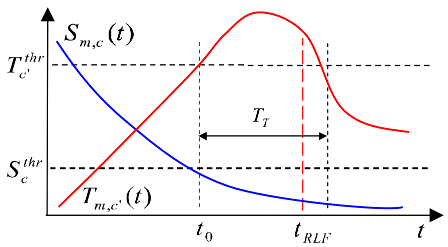

(e) Case F of TLH which can be fixed by either adjusting handover thresholds or TTT.

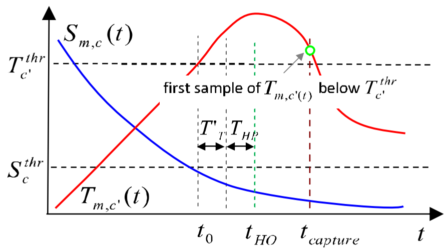

(f) The new value of TTT solving the TLH of case F.

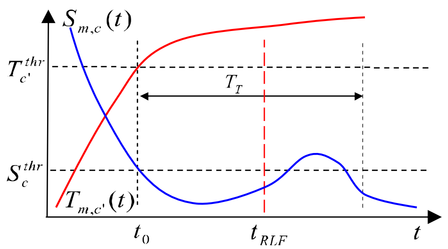

(g) Case G of TLH which can be fixed by either adjusting handover thresholds or TTT.

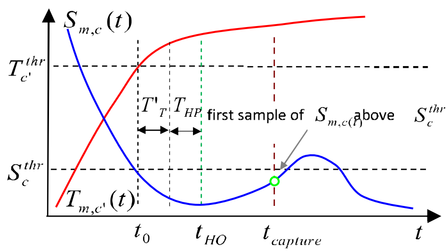

(h) The new value of TTT solving the TLH of case G.

Fig. 10 Four cases for TLH due to misconfigured TTT or handover thresholds.

2) *TEH*

Shortly after a successful inter-RAT handover from the serving cell c to target cell c', the UE drops in target cell c' due to its low SINR. One of the root causes for this TEH is the misconfiguration of the target handover threshold. An increase of $T_{c'}^{\text{thr}}$ could guarantee that the signal of the target cell of a different RAT is strong enough [10]. Another root cause is that the small value of TTT which should be increased to guarantee that the signal of the target cell c' is strong enough. The TTT could be wrongly configured in the following two cases.

Case A: After the UE is successful handed over at time instant t_{HO}, the target signal drops below the target threshold before the serving signal becomes higher than the serving threshold as shown in Fig.11(a). The UE drops in target cell c' as $T_{m,c'}(t)$ decays rapidly. In order to avoid this TEH, it is enough to delay the first handover by lengthening the TTT value. The length of the new TTT value should greater than the difference between the two instants t_0 and t_{Capture} which indicates the time instant when the first sample of $T_{m,c'}(t)$ falls below the target threshold $T_{c'}^{\mathrm{thr}}$ as shown in Fig.11(b). The prerequisite condition to consider case A as TTT-TEH KPI is defined as follows:

$$t_{\mathrm{Capture}} - t_0 \le T_{\mathrm{T}}^{\max} \tag{7}$$

$$\text{where } T_{\mathrm{T}}^{\max} = \max(I_{\mathrm{T_T}})$$

where $T_{\mathrm{T}}^{\max}$ is the largest value from the range of TTT value $I_{\mathrm{T_T}}$ in the specification defined by 3GPP.

Case B: Similar to Case A, but the length of the new TTT value should greater than the difference between the two instants t_0 and t_{Capture} which indicates the time instant when the first sample of $S_{m,c}(t)$ falls below the serving threshold S_c^{thr} as shown in Fig11(d). The precondition to consider case B as TTT-TEH KPI is defined as the same as (7) of case A.

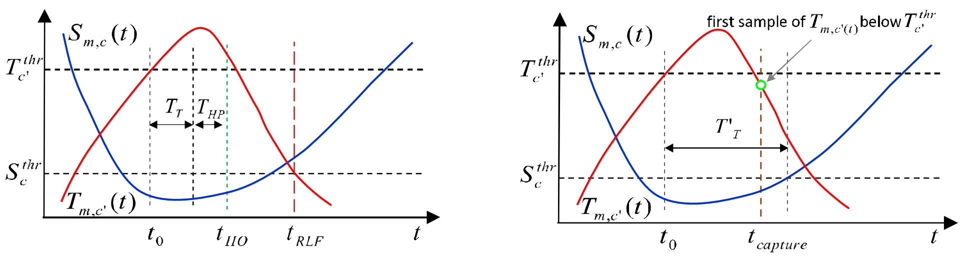

(a) Case A of TEH which can be fixed by either adjusting handover thresholds or TTT.

(b) The new value of TTT required to solve the TEH of case A.

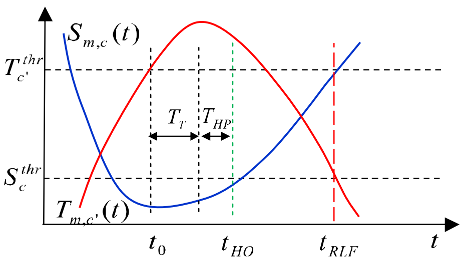

(c) Case B of TEH which can be fixed by either adjusting handover thresholds or TTT.

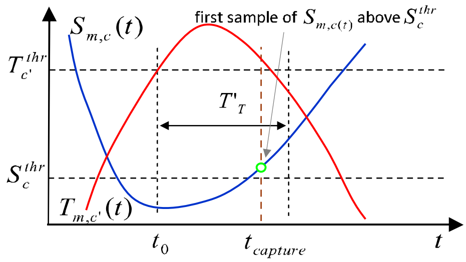

(d) The new value of TTT required to solve the TEH of case B.

Fig. 11 Two cases for TEH due to misconfigured TTT or handover thresholds.

Besides cases A and B, there is a TEH case which cannot be resolved by adjusting T_T. This case, denoted by case C, is depicted in Fig.12. Both of $S_{m,c}(t)$ and $T_{m,c'}(t)$ are stable after a successful handover. Neither a decrease nor an increase of T_{T} could avoid the execution of the first handover and the subsequent RLF. However, an increase in the target handover threshold $T_{c'}^{\mathrm{thr}}$ could avoid the first handover.

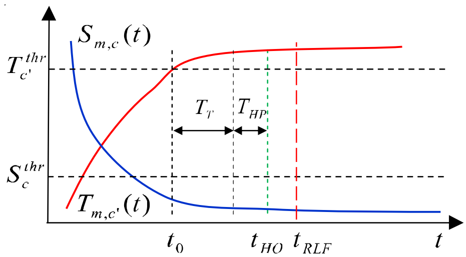

Fig. 12 An exclusive case C for TEH due to misconfigured target handover threshold.

3) *HWC*

Shortly after a successful inter-RAT handover from the serving cell c to target cell c', the UE drops in target cell c' and connects to another cell c'' which is the same RAT with cell c'. One of the root causes for this TEH is the misconfiguration of the target handover threshold. An increase of $T_{c'}^{\mathrm{thr}}$ could guarantee that the signal of the target cell of a different RAT is strong enough [10]. Another root cause is that the small value of TTT which should be increased to guarantee that the signal of the target cell c' is strong enough.

Same reason as TEHs which have been depicted in Fig.11 (a) and (c), the root cause of HWC is the misconfiguration of TTT value. In order to avoid this HWC, it is enough to delay the first handover by lengthening the TTT value. The length of the new TTT value should greater than the difference between the two instants t_0 and t_{Capture} which indicates the time instant in when the first sample of the serving or the target signal falls below its handover threshold, respectively. The prerequisite condition to consider these cases as TTT-HWC KPI is defined as same as (7) of TEH.

There is a case in HWC similarly to case C of TEH which cannot be resolved by adjusting T_{T} as shown in Fig.12. Nevertheless, increasing the target handover threshold $T_{c'}^{\text{thr}}$ could avoid the execution of the first handover and the subsequent RLF.

4) PPs

The root cause for a PP is either the misconfiguration of handover thresholds or a too small value T_{T}. Thus, similar to TEH and HWC, there is no case which is exclusive for TTT.

The first case of PP, denoted by case A, is shown in Fig.13(a). In order to avoid the first handover one of the two following actions could be used: (1) increase $T_{c'}^{\text{thr}}$ or decrease S_{c}^{thr}. (2) Increase T_T. The length of TTT should be large enough so that the first sample of the serving signal becomes higher than its corresponding threshold.

Case B shown in Fig.13(c), is similar to case A except that the signal of the target cell falls first below its corresponding threshold and later the serving signal becomes higher than the serving threshold. The prerequisite condition to consider cases A and B as TTT-PP KPI is same with (7) in TEH.

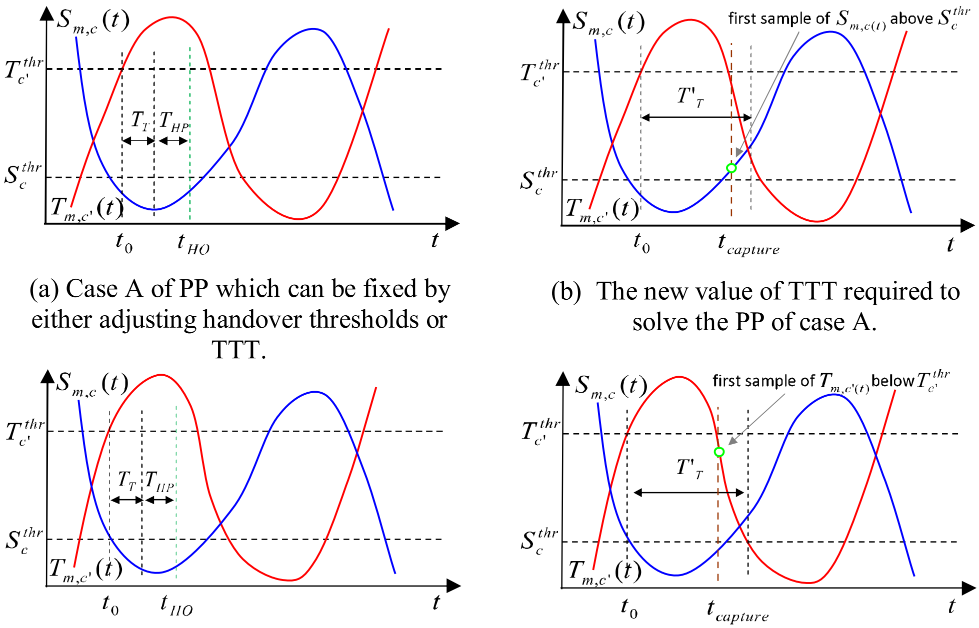

(a) Case A of PP which can be fixed by either adjusting handover thresholds or TTT.

(b) The new value of TTT required to solve the PP of case A.

(c) Case B of PP which can be fixed by either adjusting handover thresholds or TTT.

(d) The new value of TTT required to solve the PP of case B.

Fig. 13 Two cases for PPs due to misconfigured TTT or handover thresholds

5) UHs

Similar to TEH, HWC and PPs, the UHs could be avoided by delaying the handover from the higher priority RAT (LTE in our case) to the lower priority one, e.g., 3G. This can be achieved by either decreasing the serving threshold S_c^{thr} or increasing T_{T}.

The first case of UH, denoted by case A, is shown in Fig.14(a). In order to avoid the first handover one of the two following actions could be used: (1) decrease S_c^{thr}. (2) Increase T_{T}. The length of TTT should be large enough so that the first sample of the target signal becomes lower than its corresponding threshold.

Case B shown in Fig.14(c), is similar to case A except that the length of TTT should be large enough so that the first sample of the serving signal becomes higher than its corresponding threshold. The prerequisite condition to consider cases A and B as TTT-UH KPI is same with (7) in TEH.

Nevertheless, in case C when both of $S_{m,c}(t)$ and $T_{m,c'}(t)$ are stable after a successful inter-RAT handover, shown in Fig.15. Neither a decrease nor an increase of T_{T} could avoid an inter-RAT handover so as to increase the coverage of LTE cells but only by decreasing the serving handover threshold S_c^{thr}.

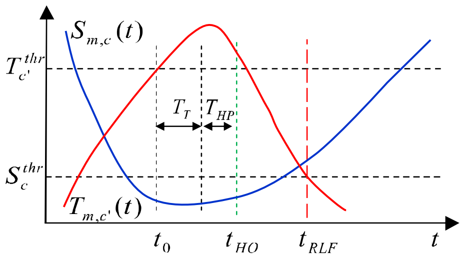

(a) Case A of root cause analysis for UHs due to a small TTT value or a high serving handover threshold.

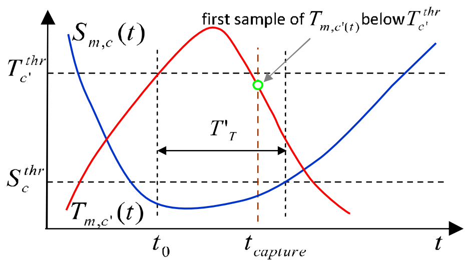

(b) Prerequisite conditions requiring a change of TTT in case A.

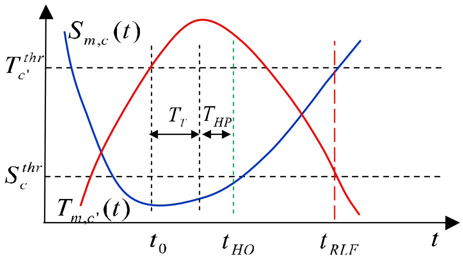

(c) Case B of root cause analysis for UHs due to a small TTT value or a high serving handover threshold.

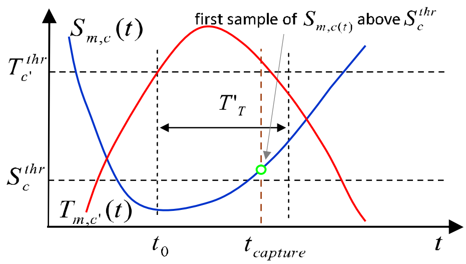

(d) Prerequisite conditions requiring a change of TTT in case B.

Fig. 14 Two root cause cases for UHs due to misconfigured TTT or handover thresholds.

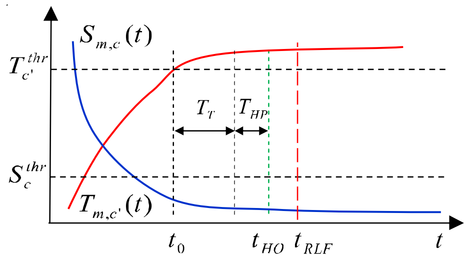

Fig. 15 An exclusive case C for UHs due to misconfigured serving handover thresholds.

4.4 *Grouping the values of the KPIs to handover threshold and TTT correction directives*

In chapter 3, we have explained how the inter-RAT KPI values are grouped into two pairs of correction directives, S_k^+ and S_k^-, T_k^+ and T_k^-, for serving and target threshold, respectively. In this section, one new pair of TTT_k^+ and TTT_k^- is introduced as correction directives for TTT parameter and which require an increase and a decrease action, respectively, in the values of TTT in the KPI period k.

4.4.1 Grouping Exclusion from UHs and PPs

The values of TTT as specified in 3GPP are not uniformly spaced [12]. The granularity of TTT is variable and tends to be larger as the value of TTT increases. For instance, the granularity between 100ms and 128ms is 28ms and the one between 640ms and 1240ms is 640ms. This increasing granularity makes it critical to group UH KPI to the correction directives of TTT. This is because changing a handover threshold with a small step size such as 1 dBm has a minor impact on the stable state. However, changing TTT to a new value with a large step size might have a critical impact on the stable mobility state, especially when there are no RLFs but a need to react on UHs.

As most operators will attempt to accept more calls into the networks while maintaining a good quality for the ones already ongoing, it is reasonable to give more priority for RLF than PPs which can be tolerated as an inevitable side effect of RLF reduction [22]. In order to ease the trade-off from decreasing or increasing the value of TTT, PP KPI is not grouped into the correction directives of TTT. Thus, the trade-off of the change of TTT value only exists in the internal KPIs of RLF. A pair of contradictive KPI groups exists in RLF as follows: (1) TLH, (2) TEH and HWC. Group 1 requires a decrease in the value of TTT for a fast handover before encountering a RLF while group 2 needs increasing TTT to avoid the first handover and the subsequent RLF.

Therefore, the correction directives of TTT exclude PP and UH KPIs. In addition, the optimization of handover thresholds provides a full solution to PP and UH. From that perspective, PPs and UHs can be completely grouped into the correction directives of handover threshold S_k^+, S_k^-, T_k^+ and T_k^-. That is, TTT is mainly utilized to resolve RLFs so as to reduce call drops and improve the user perception in terms of the uninterrupted connection.

4.4.2 The Allocation of Inter-RAT KPI Values into Correction Directives

In section 3.3, four new correction directives of handover threshold are defined as S_k^+, S_k^-, T_k^+ and T_k^-. Similarly, correction directives of TTT TTT_k^+ and TTT_k^- indicate the number of mobility failure events which require an increase and decrease, respectively, in the value of T_T in a KPI period k. The allocation between inter-RAT KPI values and six correction directives is illustrated as below.

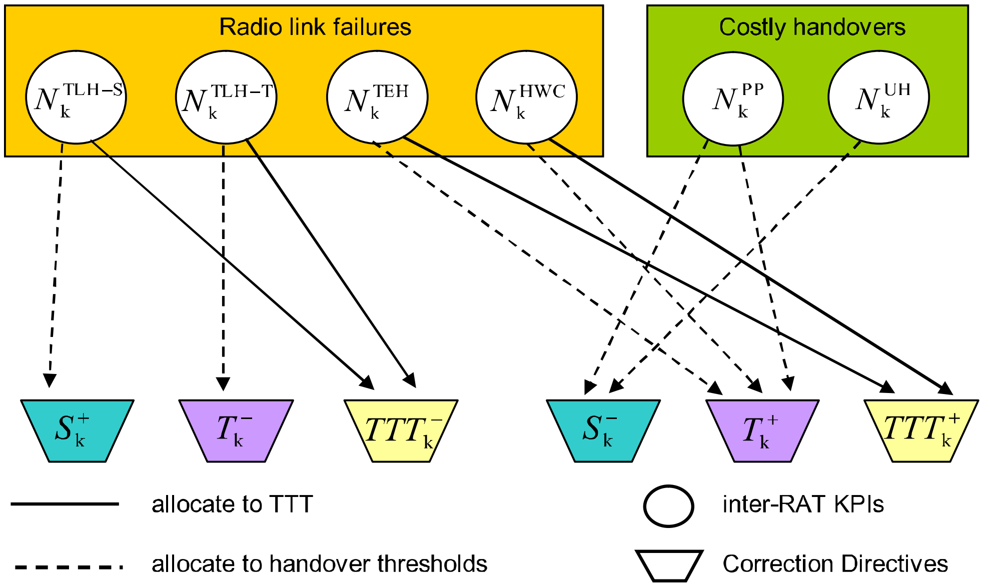

Fig. 16 Grouping the values of inter-RAT KPIs into six correction directives.

The pros and cons of introducing TTT optimization in MRO is that it provides a new degree of freedom to improve KPI performance; however, it also introduces a new difficulty in selecting one of the handover parameters to resolve mobility failure problems. As shown in Fig.16, the correction directives of handover thresholds and TTT are possible to be repetitively considered to solve the same mobility failure in some cases. On one hand, the adjustment of handover thresholds is able to resolve all mobility failure problems except for case E in TLH. As a result, most of inter-RAT KPI values can be grouped to the correction directives of handover thresholds. On the other hand, grouping inter-RAT KPI values towards TTT is conditionally considered. For instance, in the case A and B of TEH, the mobility failures are resolvable by changing either TTT or the target handover threshold. In other words, the allocation of inter-RAT KPI values is ambiguous, although there're some exclusive solutions which are only required to change either target handover threshold or TTT. In those cases, the allocation of inter-RAT KPI values is dedicated to the correction directives of one of the handover parameters.

Therefore, a grouping rule should be clarified in order to avoid uncertainty and ambiguity. We propose a reasonable strategy that TTT is considered as a prior correction directive when ambiguity of grouping occurs. This is because TTT provides a new additional degree of freedom to solve mobility problems apart from handover thresholds. On the contrary, a higher priority to change handover thresholds in this case loses an opportunity to make use of the additional parameter of TTT because most of the mobility failure problems are resolvable by handover thresholds alone. Thus, in order to utilize TTT as an additional degree of freedom to mitigate more mobility failure events, we group inter-RAT KPI values into the correction directives of TTT for the cases which are resolvable by changing the value of TTT. Otherwise, they are grouped into the correction directives of handover thresholds. The allocation priority of inter-RAT KPI values between TTT and handover thresholds is shown as below:

TABLE 1ALLOCATION PRIORITY OF INTER-RAT KPI

Solutions for Root Cause Analysis	Correction Directives	
	1st Priority	2nd Priority
Exclusive for handover thresholds	Handover thresholds	
Exclusive for TTT	TTT	
Either by handover thresholds or TTT	TTT	Handover thresholds

4.5 *Coordination between Handover Thresholds and TTT*

4.5.1 Slow and Fast Handovers

In a particular group of mobility failure events, it can be noticed that the behaviour of TTT or handover thresholds has the same impact on the change of KPIs, as illustrated in Fig.17.

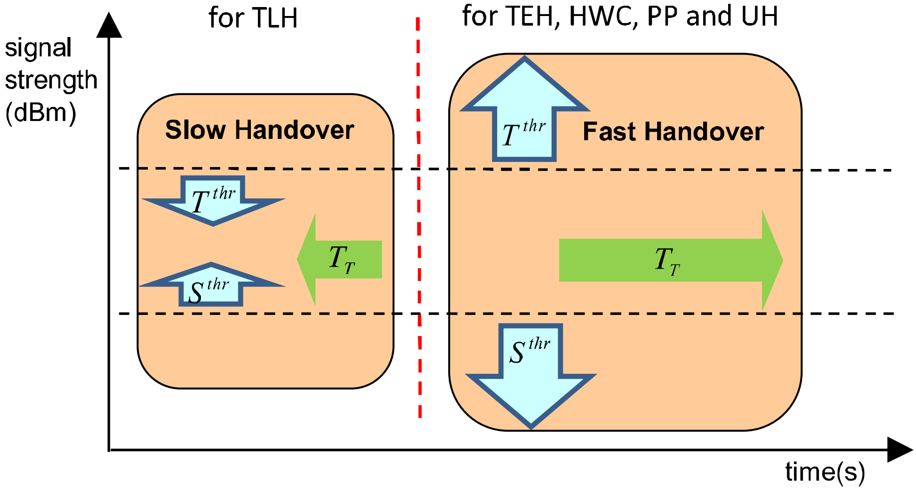

Fig. 17 Collection of correction directives for slow or fast handover.

For instance, TLH can be resolved by shortening the value of T_T or increasing serving handover threshold S^{thr} or decreasing target handover threshold T^{thr}. In the view of impact, a handover type which is called slow handover summarizes that the aforementioned changes in different handover parameters have identical influences on TLH performance. Similarly, fast handover is another handover type which has the same influences on TEH, HWC, PP and UH performance by extending the value of T_T or decreasing serving handover threshold S^{thr} or increasing target handover threshold T^{thr}.

4.5.2 Decision of Handover Parameter Controller

The role of the decision of handover parameter controller is to determine the adjusted parameter from one of the handover thresholds and TTT. As shown in Fig.17, the solution for slow handover and fast handover requires opposite change in the magnitude of handover thresholds and TTT.

Before determining which parameter to be updated, two groups of correction directives which are sorted by their handover type are evaluated. As a result of evaluation, the update of either handover thresholds or TTT should have the same impact over the KPIs in fast handover or slow handover. Eventually, the executed parameter is determined and passed to the next stage based on the magnitude of correction directives between handover thresholds and TTT. The following routine depicts how a decision of handover parameters is made.

```
Routine for making parameter decision on either handover thresholds or TTT
Input correction directives of fast handover: S^+, T^-, TTT^-
Input correction directives of slow handover: S^-, T^+, TTT^+
if sum(S^+, T^-, TTT^-) > sum(S^-, T^+, TTT^+)
    if sum(S^+, T^-) > sum(TTT^-)
        change handover thresholds
    else
        change TTT
    end if
elseif sum(S^-, T^+, TTT^+) > sum(S^+, T^-, TTT^-)
    if sum(S^-, T^+) > sum(TTT^+)
        change handover thresholds
    else
        change TTT
    end if
end if
```

Fig. 18 Routine of parameter decision

If the handover thresholds were determined, their corresponding correction directives are passed to the feedback controller. Thus, the handover thresholds are updated. If TTT was determined, its corresponding correction directives are passed to oscillation detector. If there's no oscillation, oscillation detector passes correction directives to the step controller. Otherwise, the correction directives of TTT are mapped back and combined with the correction directives of handover thresholds before both are passed to the feedback controller.

4.5.3 Cell Specific and Cell-Pair Specific Configuration Paradigm of TTT

The dual handover thresholds of measurement event B2 triggering the UE handover from LTE to 3G mobile network are configured in Cell Specific (CS) way according to current 3GPP standard [12]. An extended Cell-Pair Specific (CPS) paradigm where dual inter-RAT handover thresholds of measurement event B2 and 3A can be configured differently for each neighbouring target cell was proposed in [23]. With the same approach, the TTT of each cell can be configured in either CS or CPS way in both LTE and 3G networks.

1) CS Paradigm of TTT

In CS paradigm, a common TTT value $T_{\mathrm{T,c}}$ is used for each target neighbouring cell $c'=1,\ldots,C$. The correction directives of TTT in regard to each target cell c' are $TTT^{+}_{c,c'}$ and $TTT^{+}_{c,c'}$ which are the counters of mobility failure events that require an increase and a decrease in the TTT value, respectively. The serving cell c updates the TTT value $T_{\mathrm{T,c}}$ cell specifically based on the magnitudes of $TTT^{+}_{c,c'}$ and $TTT^{-}_{c,c'}$ which are defined as the summation of $TTT^{+}_{c,c'}$ and $TTT^{+}_{c,c'}$ of each neighbouring target cells $c'=1,\ldots,C$ as shown in equation (8) and (9).

$$TTT^{+}_{c,c'} = \sum_{c'=1}^{C} TTT^{+}_{c,c'} \tag{8}$$

$$\text{and } TTT^{-}_{c,c'} = \sum_{c'=1}^{C} TTT^{-}_{c,c'} \tag{9}$$

The handover thresholds can be configured in CPS way which is different from CS TTT. In this case, each correction directive needs to clarify its own paradigm in every step of the decision of the handover parameter as shown in Fig.18. There are two stages of quantitative comparisons where both handover thresholds and TTT are carried out in a CS way regardless of the configuration setting of handover thresholds. The first stage is on the number of comparison between the group of fast handover ($S^{+}_{c,c'}, T^{-}_{c,c'}, TTT^{-}_{c,c'}$) and the group of slow handover ($S^{-}_{c,c'}, T^{+}_{c,c'}, TTT^{+}_{c.c'}$). In this stage, the serving cell c sums up all the correction directives which are sorted by their handover type from each target cell $c'=1,\ldots,C$. The operation of each handover type is defined as follows:

$$S^{-}_{c,c'} + T^{+}_{c,c'} + TTT^{+}_{c,c'} = \sum_{c'=1}^{C} S^{-}_{c,c'} + T^{+}_{c,c'} + TTT^{+}_{c,c'} \tag{10}$$

$$\text{and } S^{+}_{c,c'} + T^{-}_{c,c'} + TTT^{-}_{c,c'} = \sum_{c'=1}^{C} S^{+}_{c,c'} + T^{-}_{c,c'} + TTT^{-}_{c,c'} \tag{11}$$

The comparison of second stage is between handover thresholds and TTT. In this stage, the correction directives of TTT and handover thresholds are performed cell specifically. For instance, ($S^{+}_{c,c'}, T^{-}_{c,c'}$) and $TTT^{-}_{c,c'}$ are defined in (9) and (12), and ($S^{-}_{c,c'}, T^{+}_{c,c'}$) and $TTT^{+}_{c.c'}$ are defined in (8) and (13).

$$S^{+}_{c,c'} + T^{-}_{c,c'} = \sum_{c'=1}^{C} S^{+}_{c,c'} + T^{-}_{c,c'} \tag{12}$$

$$\text{and } S^{-}_{c,c'} + T^{+}_{c,c'} = \sum_{c'=1}^{C} S^{-}_{c,c'} + T^{+}_{c,c'} \tag{13}$$

Three results are generated as below:

a) $(S^{+}_{c,c'}, T^{-}_{c,c'}) > TTT^{-}_{c,c'}$ or $(S^{-}_{c,c'}, T^{+}_{c,c'}) > TTT^{+}_{c,c'}$. In this case, $(S^{+}_{c,c'}, T^{-}_{c,c'})$ or $(S^{-}_{c,c'}, T^{+}_{c,c'})$ is dominant and implies that most of the mobility failure events are caused by misconfigured handover thresholds. As a result, the serving cell c updates the handover thresholds S^{thr}_{k} and T^{thr}_{k} in a CS or CPS way according to current configuration setting. For instant, in the case of CS, the same magnitude of change is performed on the handover thresholds with respect to each neighbouring cell $c' = 1, \ldots, C$. Whereas in the case of CPS, the magnitude of change performed on the handover thresholds can be different with respect to different neighbouring cell c'.

b) $(S^{+}_{c,c'}, T^{-}_{c,c'}) < TTT^{-}_{c,c'}$ or $(S^{-}_{c,c'}, T^{+}_{c,c'}) < TTT^{+}_{c,c'}$. In this case, $TTT^{-}_{c,c'}$ or $TTT^{+}_{c.c'}$ is dominant and implies that most of the mobility failure events are caused by misconfigured value of TTT. As TTT is configured cell specifically, the TTT value $T_{\mathrm{T,c}}$ is updated with the same magnitude of change with respect to each neighbouring cell c'.

c) $(S^{+}_{c,c'}, T^{-}_{c,c'}) \approx TTT^{-}_{c,c'}$ or $(S^{-}_{c,c'}, T^{+}_{c,c'}) \approx TTT^{+}_{c,c'}$. In the last case, no obvious correction directives are dominant and consequently the serving cell c updates neither the handover thresholds nor the TTT value.

2) CPS Paradigm of TTT

In contrast to CS paradigm, different TTT values $T_{\mathrm{T},c,c'}$ are used for each target neighbouring cell $c' = 1, \ldots, C$. The correction directives of TTT in regard to each target cell c' are $TTT^{+}_{c,c'}$ and $TTT^{-}_{c,c'}$. The serving cell c updates the TTT value $T_{\mathrm{T,c,c'}}$ cell-pair specifically based on the magnitudes of $TTT^{+}_{c,c'}$ and $TTT^{-}_{c,c'}$ in regard to each neighbouring target cells $c' = 1, \ldots, C$ as shown in (14) and (15).

$$TTT^{+}_{c,c'} = TTT^{+}_{c,c'} \tag{14}$$

$$\text{and } TTT^{-}_{c,c'} = TTT^{-}_{c,c'} \tag{15}$$

Both of handover thresholds and TTT can be configured in a CPS way. In Fig.18, during the first stage of comparison between the group of fast handover ($S^{+}_{c,c'}$, $T^{-}_{c,c'}$, $TTT^{-}_{c,c'}$) and the group of slow handover ($S^{-}_{c,c'}, T^{+}_{c,c'}, TTT^{+}_{c.c'}$), the serving cell c only collects the correction directives from a single target neighbouring cell c'.

$$S^{-}_{c,c'} + T^{+}_{c,c'} + TTT^{+}_{c,c'} = S^{-}_{c,c'} + T^{+}_{c,c'} + TTT^{+}_{c,c'} \tag{16}$$

$$\text{and } S^{+}_{c,c'} + T^{-}_{c,c'} + TTT^{-}_{c,c'} = S^{+}_{c,c'} + T^{-}_{c,c'} + TTT^{-}_{c,c'} \tag{17}$$

The comparison of second stage between handover thresholds and TTT are performed cell pair specifically. For instance, ($S^{+}_{c,c'}, T^{-}_{c,c'}$) and $TTT^{-}_{c,c'}$ are defined in (15) and (18), and ($S^{-}_{c,c'}, T^{+}_{c,c'}$) and $TTT^{+}_{c.c'}$ are defined in (14) and (19).

$$S^{+}_{c,c'} + T^{-}_{c,c'} = S^{+}_{c,c'} + T^{-}_{c,c'} \tag{18}$$

$$\text{and } S^{-}_{c,c'} + T^{+}_{c,c'} = S^{-}_{c,c'} + T^{+}_{c,c'} \tag{19}$$

Three generated results are similar to those in CS paradigm but executed in a CPS way.

4.6 *Step-wise Time-to-Trigger Joint Optimization*

In the step controller, the step size of TTT is defined by the specification of 3GPP in [12]. $T_{\mathrm{T},k-1}$ is updated to a new value $T_{\mathrm{T},k}$ by adding a step value G_k within the defined range of TTT based on the magnitude of its corresponding correction directives TTT^{+}_{k} and TTT^{-}_{k} in each KPI period as shown in Fig.19. For instance, $T_{\mathrm{T},k-1}$ is increased if the magnitude of TTT^{+}_{k} is higher than TTT^{-}_{k}. On the contrary, $T_{\mathrm{T},k-1}$ requires a decrease if the magnitude of TTT^{-}_{k} is higher than TTT^{+}_{k}. The value of T_{T} is updated as follows:

$$T_{\mathrm{T},k} = T_{\mathrm{T},k-1} + G_k \tag{20}$$

$$\text{and } T_{\mathrm{T},k} = T_{\mathrm{T},k-1} - G_k \tag{21}$$

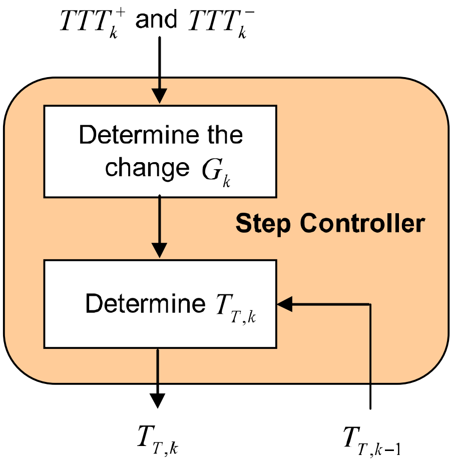

Fig. 19 Step controller with the change defined in 3GPP.

The updated TTT value $T_{\mathrm{T},k}$ is fed into the networks and its adjustment is repeated until the stable state is reached or the optimization of TTT is stopped when its value consecutively oscillates.

The step-wise approach for TTT optimization reduces the number of mobility problems due to misconfigured TTT. However, it may require many KPI periods for the repetitive process until the mobility problems due to inappropriate TTT are resolved. In the next section, we'll propose a new approach that TTT is changed in a stepless manner.

4.7 *Stepless Time-to-Trigger Joint Optimization*

4.7.1 The Measurement of TTT

In chapter 4, the root cause of all cases from each KPI has been analyzed. In those cases where mobility failure events are considered as a result of misconfigured TTT, a proper value of TTT can be found and updated so that the UE can avoid mobility failure events. As the correction directives of TTT are excluded from PP and UH, the measurements of TTT value are only applied to TLH, TEH and HWC.

3) TLH

The four TLH cases denoted by case D, E, F and G have been shown in Fig.10. Cases D and E have same measurement policy whereas case F and G have another same measurement policy.

Case D and E: This RLF can be avoided by shortening TTT interval T_{T} until the handover to target cell c' which can be completed just before RLF occurs. The proper TTT interval T_{T} and the handover preparation time interval T_{HP} should be one time instant less than the elapse between the two time instants t_{RLF} and t_0. The measured TTT value $T_{\mathrm{T},k}$ is updated and defined in (22).

$$T_{\mathrm{T},k} = t_{\mathrm{RLF}} - t_0 - T_{\mathrm{HP}} - 1 \tag{22}$$

Case F and G: The TTT interval T_{T} and handover preparation time interval T_{HP} should be one time instant less than the elapse between the time instant t_{Capture} and t_0. In this case, the handover to target cell c' is executed and a RLF at t_{RLF} is avoided. The measured TTT value $T_{\mathrm{T},k}$ is updated and defined in (23):

$$T_{\mathrm{T},k} = t_{\mathrm{Capture}} - t_0 - T_{\mathrm{HP}} - 1 \tag{23}$$

4) TEH and HWC

Both TEH and HWC has the same root cause that is the small value of TTT which should be increased to guarantee that the signal of the target cell c' is strong enough as depicted in Fig.11.

Case A and B: In order to avoid TEH and HWC, it is enough to delay the first handover by lengthening the TTT value. The new TTT value $T_{\mathrm{T},k}$ should be of equal length between the two instants t_0 and t_{Capture}. The measured TTT value $T_{\mathrm{T},k}$ is updated and defined in (24):

$$T_{\mathrm{T},k} = t_{\mathrm{Capture}} - t_0 \tag{24}$$

4.7.2 Step Controller and Storage Pool for TTT

The measurement of TTT is used to update the TTT value to a proper one which solves the RLF that happens to the UE. From the perspective of implementation, this measurement is reported to the base station by the UE and the decision is made by the base station. In the uplink, UE measure an appropriate length of TTT value in a report for serving cell and inter-RAT neighboring handover target cells. As a result, each UE m has different measured TTT values $T_{\mathrm{T},k}^{m}$ to resolve its own mobility failure problems in KPI period k. However, in the downlink, the serving cell in LTE or 3G network configures each connected UE with the same TTT value. In order to reduce more mobility failure problems, the selected TTT value from all the measured candidates should be the one that is proposed the most frequently by all the UEs via measurement reports. The structure of stepless controller is shown as below:

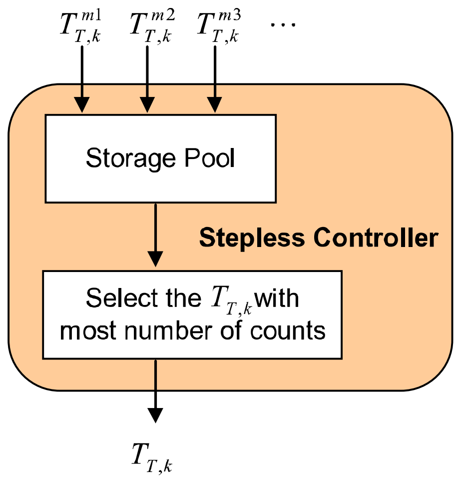

Fig. 20 Stepless controller consisting of a storage pool to save all measured TTT values for each UE.

4.8 Convergence Aspect of the New SON-based Algorithm

With step controller to update TTT value and feedback controller to update handover thresholds, a cell achieves stable state when the magnitude of the same pair of correction directives are either similar or equal to each other or lower than the thresholds $S^{\min}$, $T^{\min}$ and $TTT^{\min}$ as shown in Fig.21.

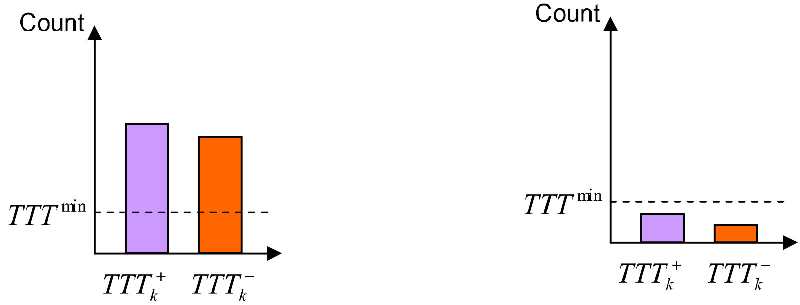

(a) TTT_k^{+} and TTT_k^{-} are similar or equal.

(b) TTT_k^{+} and TTT_k^{-} are below $TTT^{\min}$.

Fig. 21 Two examples of the stability of a cell depending on TTT.

4.8.1 Oscillation Detector for TTT

However, a cell may not reach stability as one of aforementioned cases. For instance, an increase of T_T according to a large magnitude of TTT_k^+ may cause a decrease of T_T which is required by the increasing TTT_k^- as showed in Fig.22(a). Vice versa, the values of TTT oscillate when T_T increases after a decrease in the previous KPI period. The latter oscillation pattern of TTT is depicted in Fig.22(b). Thus, the oscillation of TTT is defined and counted by its changing pattern. In this case, the value of TTT is being constantly updated up and down in each KPI period and the stability is not achieved.

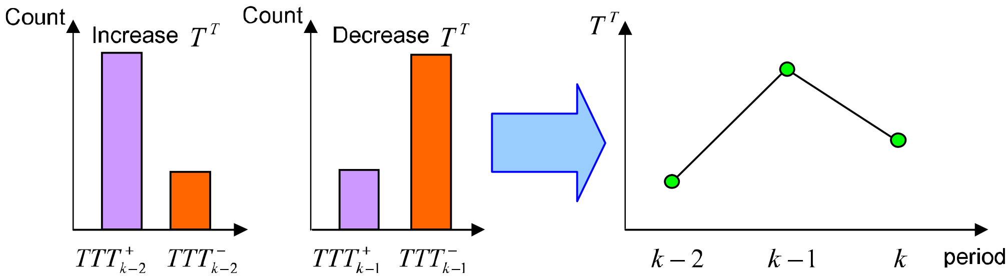

(a) T_T increases and then decreases from KPI period k-2 to k.

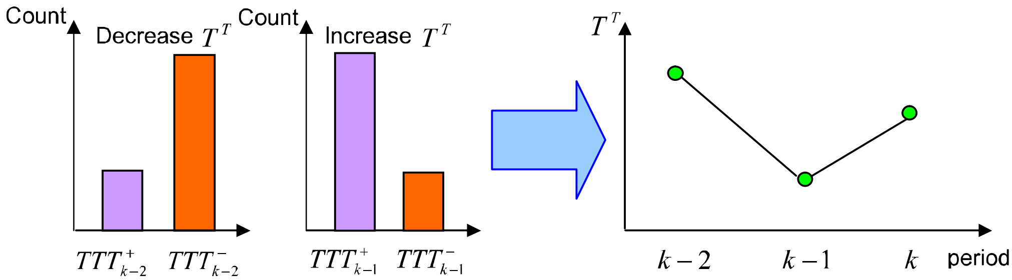

(b) T_T decreases and then increases from KPI period k-2 to k.

Fig. 22 Two types of oscillation pattern of TTT

The oscillation detector is highlighted in Fig.23. When there's no TTT oscillation detected, the current TTT value is passed to step controller for the next TTT optimization. If two consecutive TTT oscillations are detected by oscillation detector, in order to maintain the stability of a cell TTT optimization needs to be stopped. As a result, all mobility failure events which are grouped into TTT are mapped back to the correction directives of handover thresholds via a mapback controller and then passed to feedback controller for the optimization of handover thresholds. On the other hand, the value of TTT is selected from one of the values in the latest two KPI periods $k-1$ and k. That is, for those cells which undergo TTT oscillations their optimization is performed only in regard to handover thresholds and taking into account the selected TTT value with all mobility failure events including those derived from TTT.

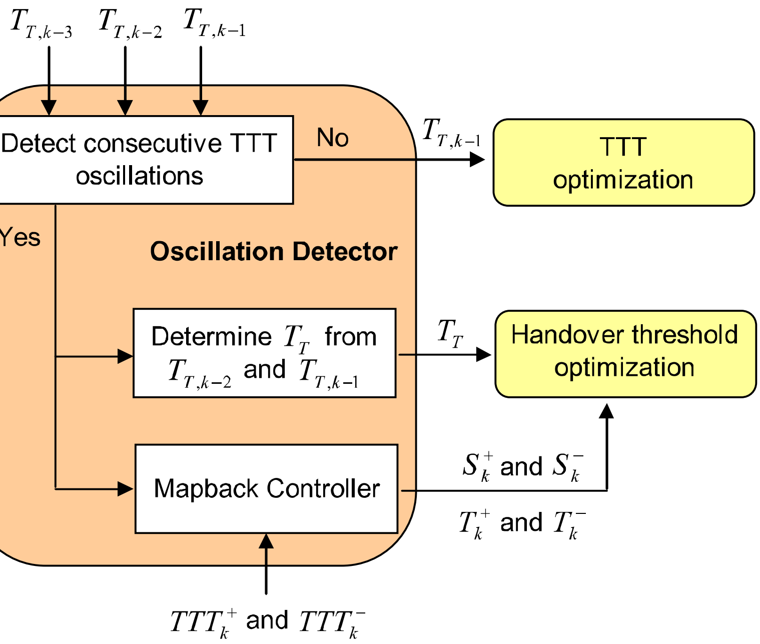

Fig. 23 Description of oscillation detector before TTT and handover threshold optimization.

4.8.2 Selection of TTT Value during Oscillations

The value of TTT is selected when TTT optimization is stopped during TTT oscillation. To find an appropriate value of TTT we investigate the trend of performance change in order to reach a closer global optimum performance. Followings are couple of strategies concerning the global optimum performance in a cell by selecting a proper value of TTT between the current and previous KPI periods.

In the thesis study, the difficulty to reach minimum mobility failure event in a cell is how to deal with a trade-off between slow handover and fast handover, because they require a contradictory change in the magnitude of T^{thr}. For instance, T^{thr} needs to be decreased to reduce TLH-T in slow handover while T^{thr} needs to be increased to reduce TEH, HWC and PP in fast handover. On the other hand, without too much trade-off, increasing S^{thr} reduces TLH-S and most of the time UH is ignored when TLH is non-zero. Nevertheless, increasing S^{thr} may lead to a rise in the number of TLH-T or other KPIs in fast handover. In this case, the number of TLH-S which requires an increase of S^{thr} is a significant clue to select the TTT value in one of the KPI periods $k-2$ and $k-1$. Followings are two cases depending on the number of TLH-S.

1) TLH-S is small in the latest two KPI periods as depicted in Fig.24, that is, other mobility failure problems such as TLH-T, TEH, HWC and PP are major issue. The oscillation between TLH-T and fast handover occurs because T^{thr} is required to constantly change up and down in each KPI period. In this case, we take the value of TTT in the KPI period when the number of overall mobility failure events is minimal.

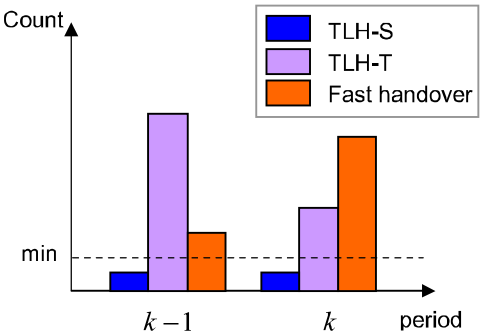

Fig. 24 KPI performances when TLH-S is small.

2) If TLH-S is large in the latest two KPI periods as depicted in Fig.25, take the value of TTT when fast handover is more than TLH-T considering the following three reasons:

a. Decreasing TLH-S may generate new contradictory issue between TLH-T and fast handovers. In other words, TLH-S cannot be considered as a determination factor for the minimization of overall mobility failure events and TTT selection.
b. Holding a larger number of fast handover implies that the current value of TTT is too short and the number of TLH-T is relatively small.
c. Increasing T^{thr} guarantees that the signal strength of target handover cells is strong enough. On some extent, the quality is assured and benefits more from increasing T^{thr} compared with decreasing T^{thr}.

A summary from the above three points is that with a shorter TTT the fast handover problems can be resolved by increasing T^{thr} and meanwhile

TLH-T is controlled under a relative low number regardless of the decline of TLH-S.

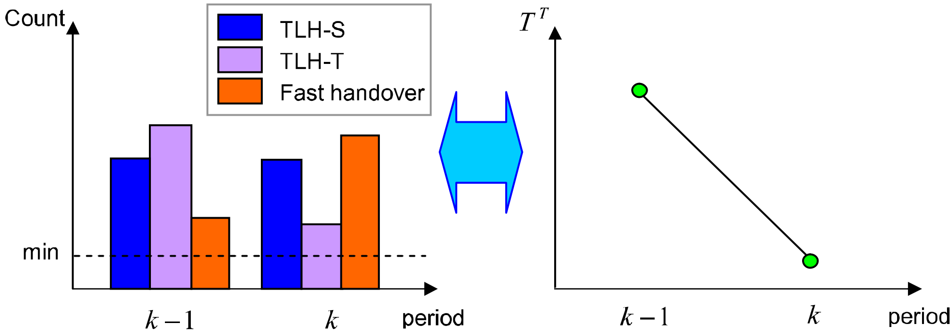

Fig. 25 KPI performances when TLH-S is large and the corresponding TTT values.

By this way, the contradictory change on T^{thr} can be resolved by taking TTT into account as a new degree of freedom and thus the closer global optimum performance is achieved.

CHAPTER 5
Simulation Scenario and Results

In the first phase of LTE deployment, the new LTE mobile system will focus on the areas with high user traffic throughput and overlay the pre-existing mobile system which in our case is 3G system. There're some spots called coverage holes where the coverage does not exist in one of the RAT, such as downs of the terrain, indoor of the building. As a result, the limited LTE coverage or coverage holes will yield many inter-RAT handovers from LTE to 3G and vice versa. In this chapter there's one academic scenario to be investigated: fully overlaying LTE and 3G networks. In addition, in order to investigate the inter-RAT handover optimization in approximate real-life networks, we will present the simulation results through an extra scenario which is partly overlaying LTE network on top of 3G network in appendix section.

5.1 *Scenarios and Simulation Parameters of LTE and 3G Networks*

In this section the fully overlaying networks scenario is introduced with simulation parameters of LTE and 3G networks and inter-RAT MRO algorithm with handover thresholds combining TTT optimization.

The complete area including urban and suburban is served by both LTE cells in blue and 3G cells in red as shown in Fig.26. The hexagonal cell borders of LTE and 3G networks are fully overlapped. The network-wide number of co-located sites is 7 with totally 42 sectorized cells among which are 21 LTE cells and 21 3G cells. The frequency band set for LTE and 3G is 2.6 GHz and 2.1 GHz, respectively.

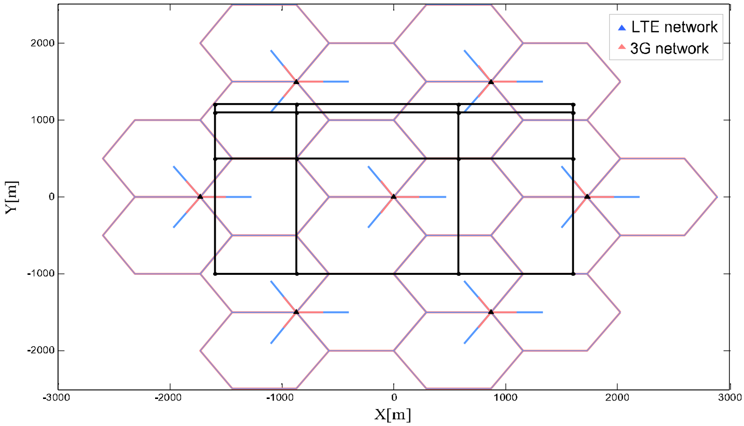

Fig. 26 Network layout of LTE and 3G and street loops in fully overlaying networks scenario.

The KPI collection period T_{KPI} for both LTE and 3G networks are set to a small value of 150s to reduce computational complexity. On the other hand, in order to collect enough number of mobility failure events to improve the accuracy of the change of parameters, it's necessary to activate a large number of UEs in the networks. In this case, a total number of 1010 UEs are distributed in the background and the street loops. There're 5 background UEs in each cell which are moving randomly at a low speed of 3km/h inside the network borders and 800 street UEs which are moving fast at various speeds along the specific street loops in black plot in Fig.26. The Shadow fading is modeled by a log-normal random variable with 0 dB mean and 8 dB standard deviation. To investigate the inter-RAT reaction against the mobility robustness, the traffic steering strategy is not used. Therefore, the shadow fading is generated to be uncorrelated for each radio link between two RATs. The fast fading is modeled using Jake's model [24] and 2-ray Rayleigh fading channel assuming the frequency diversity order is 2. The handover measurements are averaged incoherently by Layer 1 (L1) filter [25]. After that, a log-normally distributed measurement error is introduced in the filtered handover measurement [26]. The updated measurement results are processed by a Layer 3 (L3) filter applying a filter coefficient of 4-default value for inter-RAT measurements [12]. The handover event is triggered based on the measurement event conditions which are evaluated by the processed measurement of L3, i.e. RSRP in LTE and RSCP in 3G. The parameters for simulation and algorithm are listed in Table 2.

TABLE 2 SIMULATION AND ALGORITHM PARAMETERS

Parameter	Assumptions	Inter-RAT MRO Algorithm	
Number of Cells	LTE: 21 and 3G: 21	T_{KPI}	150 s
Carrier frequency	LTE: 2.6 GHz and 3G: 2.1 GHz	T_T	0.1 s, 0.128 s, 0.256 s,
System Bandwidth	LTE: 10 MHz and 3G: 5 MHz		0.32 s, 0.48 s, 0.512 s,
Total transmit power	LTE: 40 W and 3G: 20 W		0.64 s, 1.024 s, 1.28 s,
Shadowing	Standard deviation = 8 dB		2.56 s, 5.12 s
	Decorrelation distance = 50 m	T_{HP}	0.25 s
	Correlation between BSs = 0.5	$T_{Q_{fail}}$	0.5 s
	Correlation between sectors = 1	Q_{fail}	-8 dB
	Correlation between RATs = 0		
Fast fading	2-ray Rayleigh fading channel		
Measurement bandwidth	RSRP: 1.25 MHz and RSCP: 5 MHz		
L3 measurement filtering	Filter coefficient = 4		
Number of UEs	Background: 5 per cell		
	Street: 800		
UE speed	Background: 3 km/h		
	Street: 30km/h, 60km/h, 90km/h, 120km/h		

5.2 *Simulation Results*

Firstly, the inter-RAT MRO algorithm for jointly self-optimizing handover thresholds and TTT is evaluated in two approaches: step-wise and stepless change of TTT value. Secondly, the inter-RAT handover thresholds and TTT are configured with different paradigms.

5.2.1 Evaluation Methodology

According to the performance investigation of various configuration paradigms of dual handover thresholds S^{thr} and T^{thr}, it was proposed that the threshold of serving cell S^{thr} is better to be configured in a cell-specific manner[23], and T^{thr} is configured in a CPS way. In this thesis, we focus on 6 different configuration paradigms with the coordination of TTT and handover thresholds as depicted in table 3. The network-wide (NW) setting is a common value which is for all cells within the same network and is used for benchmarking.

TABLE 3 SIX CONFIGURATION PARADIGMS FOR THE COORDINATION OF INTER-RAT HANDOVER THRESHOLDS AND TTT

Paradigm	Handover Threshold		TTT
	S^{thr} and	T^{thr}	T_{T}
1	NW	NW	NW
2	CS	CS	NW
3	CS	CS	CS
4	CS	CPS	NW
5	CS	CPS	CS
6	CS	CPS	CPS

According to performance criteria, we denote the total number of TLH-S, TLH-T, TEH, HWC, PP and UH in LTE network by $N_{\text{TLH-S}}^{\text{LTE}}$, N_{TLH-T}^{LTE}, N_{TEH}^{LTE} ,N N_{HWC}^{LTE}, $N_{\text{PP}}^{\text{LTE}}$, $N_{\text{UH}}^{\text{LTE}}$ and 3G network by $N_{\text{TLH-S}}^{\text{3G}}$, N_{TLH-T}^{3G}, N_{TEH}^{3G}, N_{HWC}^{3G} $N_{\text{PP}}^{\text{3G}}$, respectively, $N_{\text{UH}}^{\text{3G}}$ is excluded in 3G. The total number of RLFs per cell is summed up by its related KPI values, and is denoted by N_{RLF}^{k} in KPI period k as shown in (25).

$$N_{RLF}^{k} = N_{TLH-T}^{k} + N_{TLH-S}^{k} + N_{TEH}^{k} + N_{HWC}^{k} \tag{25}$$

In order to evaluate the whole performance of inter-RAT MRO algorithm in two different networks, the total numbers of mobility failure events are simplified and calculated as follows:

$$N_{RLF} = N_{RLF}^{LTE} + N_{RLF}^{3G} \tag{26}$$

$$N_{PP} = N_{PP}^{LTE} + N_{PP}^{3G} \tag{27}$$

$$N_{UH} = N_{UH}^{LTE} \tag{28}$$

In order to have a scientific and easy method to benchmark different optimized KPIs of overall network performance induced by various configuration paradigms, we defined a cost function to investigate RLFs, PPs and UHs whether they achieve a lower number of mobility failure events in both LTE and 3G networks. The cost function z is defined as follows:

$$z = N_{RLF} + w_p \cdot N_{PP} + w_u \cdot N_{UH} \tag{29}$$

$z = N_{RLF} + N_{PP}$, When $w_p = 1$, $w_u = 0$

Where w_p and w_u are weight used for the total number N_{PP} of PPs in both LTE and 3G and N_{UH} of UHs in only LTE, respectively. As RLFs and PPs are easily perceived by users through call drops, background noise, and intermittent voice etc, which has more direct impacts on user-perceived quality comparing to UHs. Further more, UHs require an opposite adjustment against TLH-S on handover threshold which leads to a negative impact to the number of RLFs. Hence, a same higher weight for RLFs and PPs are attributed to the cost function while lower weight is set for UHs, i.e. $w_p = 1, w_u = 0$.

5.2.2 Comparison between the Performance of the Inter-RAT MRO with Step-wise and Stepless TTT Optimization

The extended inter-RAT MRO algorithm including TTT into account is capable of finding an appropriate TTT value which can resolve most of mobility failure events after certain number of KPI periods. This number of required KPI periods is mainly decided by the number of TTT steps and the complexity of reducing overall mobility failure events by jointly optimizing handover thresholds and TTT value. In chapter 4.7, a new stepless approach was introduced to reduce the KPI periods for the repetitive process of TTT optimization due to setting an inappropriate TTT value.

In this section, the simulation results are investigated under network-wide setting, CS step-wise TTT and CS stepless TTT settings. The network-wide setting is used to benchmark the performance of different inter-RAT MRO paradigms with handover thresholds and TTT optimization. The initial values for handover thresholds are same in all sex configuration paradigms: S^{thr} = -110 dBm and T^{thr} =-104 dBm are configured for the measurement event B2 and 3A in LTE and 3G, respectively. In Fig.27, the total number of RLFs, PPs and UHs in LTE and 3G networks is denoted by N_{RLF}, N_{PP} and N_{UH}, respectively, for each initial TTT setting. The UE moving on the street has four varied speeds which are set to 30km/h, 60km/h, 90km/h and 120km/h for investigating the best TTT value in each speed. All simulation results are obtained by using Matlab.

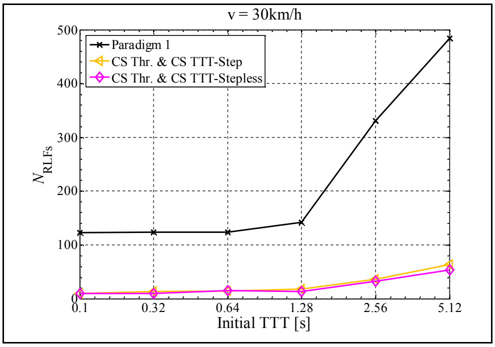

(a) Numbers of RLF in 3G and LTE cells at 30km/h

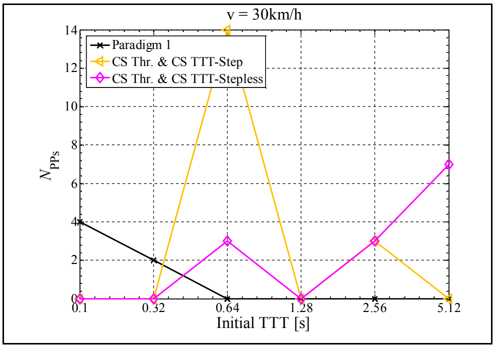

(b) Numbers of PP in 3G and LTE cells at 30km/h

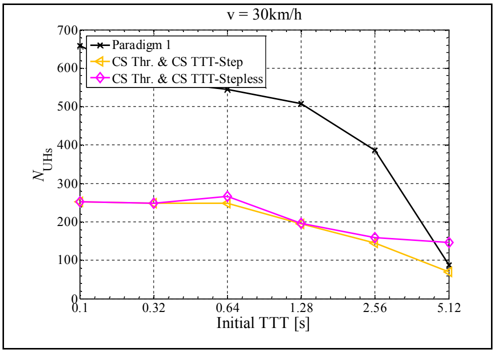

(c) Numbers of UH in 3G and LTE cells at 30km/h

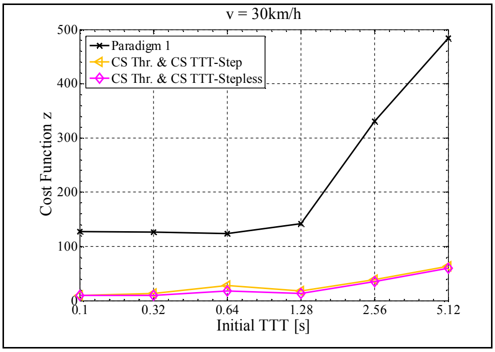

(d) Cost Function in 3G and LTE cells at 30km/h

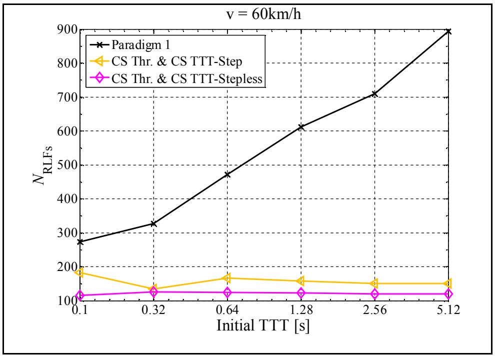

(e) Numbers of RLF in 3G and LTE cells at 60km/h

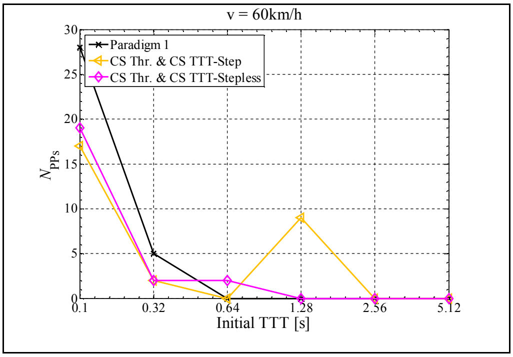

(f) Numbers of PP in 3G and LTE cells at 60km/h

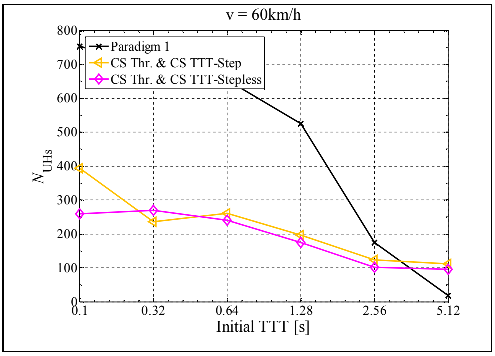

(g) Numbers of UH in 3G and LTE cells at 60km/h

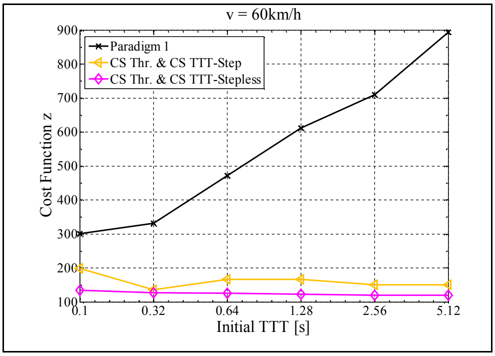

(h) Cost Function in 3G and LTE cells at 60km/h

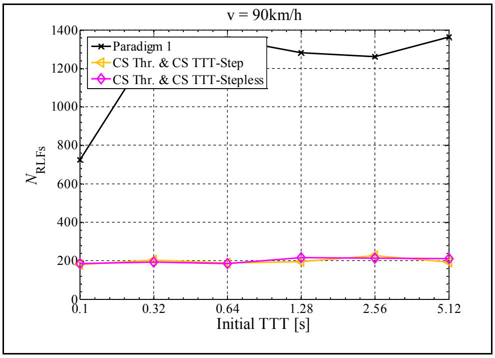

(i) Numbers of RLF in 3G and LTE cells at 90km/h

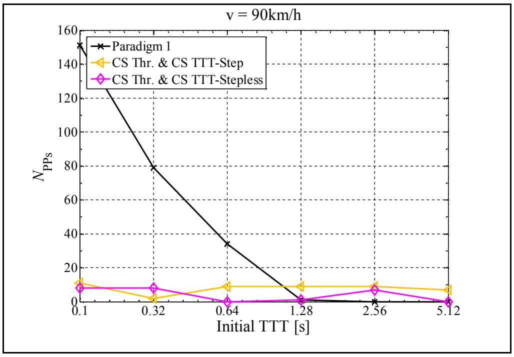

(j) Numbers of PP in 3G and LTE cells at 90km/h

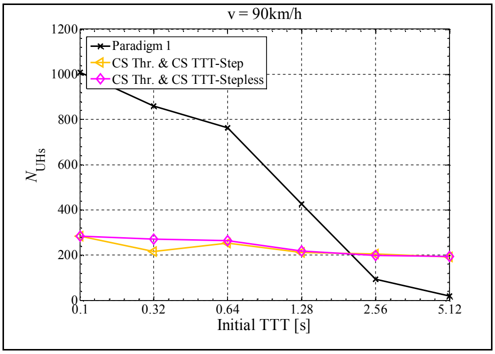

(k) Numbers of UH in 3G and LTE cells at 90km/h

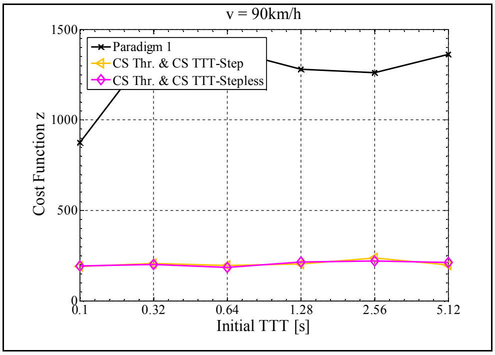

(l) Cost Function in 3G and LTE cells at 90km/h

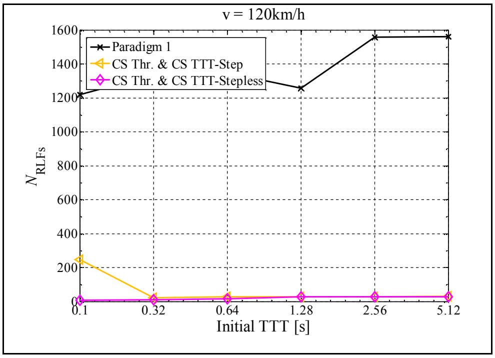

(m) Numbers of RLF in 3G and LTE cells at 120km/h

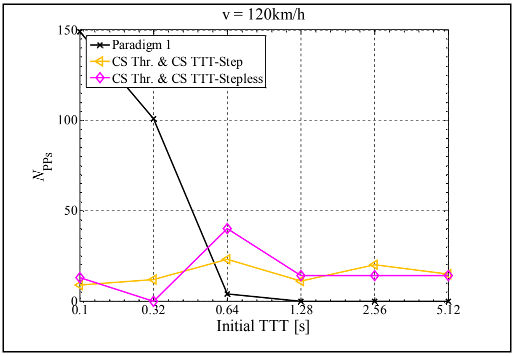

(n) Numbers of PP in 3G and LTE cells at 120km/h

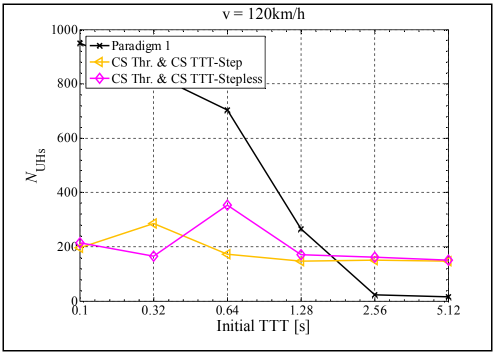

(o) Numbers of UH in 3G and LTE cells at 120km/h

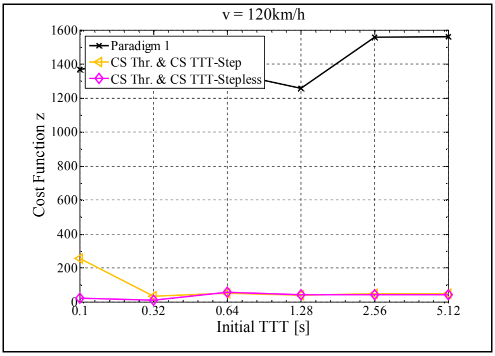

(p) Cost Function in 3G and LTE cells at 120km/

Fig. 27 Comparison between the overall performance of the network-wide settings and 2 TTT optimized approaches

In Fig.27(d), Fig.27(h), Fig.27(l) and Fig.27(p), the cost function decline substantially by applying the CS paradigms in contrast to NW paradigm. This is because the NW setting is a common value for all cells while in CS paradigm a common value is used for each target neighbouring cell. In other words, CS paradigm offers more flexibility than NW paradigm to solve more mobility failure events by setting different target neighbouring cells a specific value instead of a universal one.

The difference between step-wise and stepless TTT optimization is not as much as that was present between NW and CS paradigms. In the cost function plots at speed 60km/h and 120km/h, it is shown that the performance of stepless TTT paradigm is slightly lower than that achieved by step-wise TTT paradigm, while N_{UH} achieved by both CS TTT paradigms are generally the same. From the perspective of implementation, base station decides the selected TTT value from all measured candidates reported by all the UEs in the uplink. By resolving the most frequent mobility failure events grouped by misconfigured TTT value in one KPI period it avoids the possibility of oscillations occurs when many candidates are set one after another in many KPI periods. Without oscillation TTT is not mapped back to the correction directives of handover thresholds by the oscillation controller. Thus, this slight decrease in cost function using stepless TTT paradigm is justified by avoiding oscillation and utilizing TTT as the additional degree of freedom to resolve more mobility failure problems. In the following section, stepless TTT approach will be used by default in both CS and CPS TTT optimization paradigms.

5.2.3 Comparison between the Performance of the Inter-RAT MRO Algorithm without and with TTT Optimization

In this section, we compare the performance of the MRO algorithm with respect to a network-wide setting for benchmarking reference paradigm 1, and five paradigms 2-5 in the form of different combined configuration of inter-RAT handover thresholds and TTT.

In the cost function at lower speed 30km/h plotted in Fig.28(d), paradigms 2-5 which are configured in either CS or CPS manner achieve a large gain from the network-wide paradigm 1 which uses the same parameter for all cells. Paradigm 3 which optimizes the inter-RAT handover thresholds and TTT both in a CS way outperforms paradigm 2 because paradigm 2 is only optimized by handover thresholds in a CS way and all cells are configured with the same TTT value. As it's shown in Fig.28(d), the larger initial TTT value is the bigger performance gain will achieve. For example, at the largest initial TTT value 5.12s, paradigm 3 even achieves a gain of 67% compared to paradigm 2. The reason is that firstly there's one case in TLH which is exclusively resolved by TTT, and secondly TTT provides an additional degree of freedom to avoid oscillation that the dual handover thresholds cannot resolve alone. Paradigm 4 that configures the second threshold of measurement event B2 and 3A in a CPS manner outperforms paradigm 2 which configures handover thresholds in a CS manner. Paradigm 5 has less mobility failure problems than paradigm 4 as CS TTT optimization is introduced. Paradigm 5 has the best performance over other 5 paradigms including paradigm 6 on the cost function because configuring different TTT values for each target neighbouring cell in a CPS way may cause over adjustment and wrong decision by setting an inappropriately recommended TTT value. The gain scheduler of handover thresholds allows reducing the magnitude of the second threshold of measurement event B2 and 3A to a smaller value which is 0.1dB in our case. However, the range of TTT values defined by 3GPP doesn't have an equal interval and small gradient as handover thresholds. For instance, there's no such an intermediate value between 2.56s and 5.12s to be taken properly when an increase of TTT value to 3s is demanded. As a result, 5.12s will be decided to be used from a changing request and it may result in a decline of overall KPI performance.

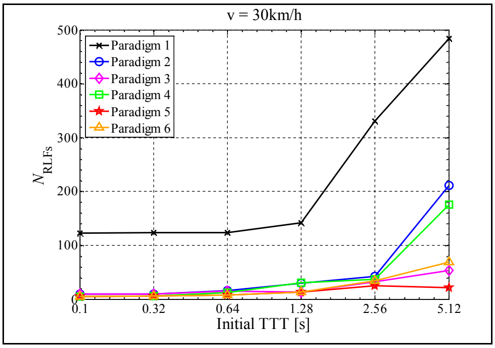

(a) Numbers of RLF in 3G and LTE cells at 30km/h

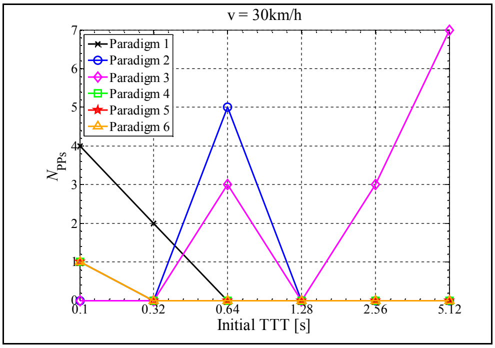

(b) Numbers of PP in 3G and LTE cells at 30km/h

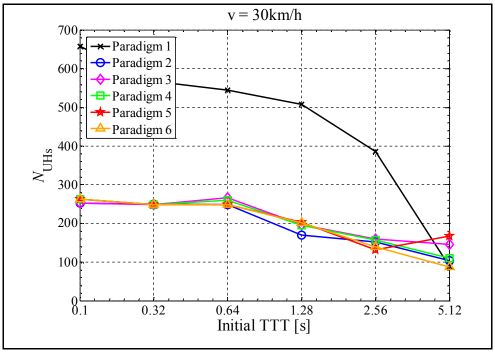

(c) Number of UH in 3G and LTE cells at 30km/h

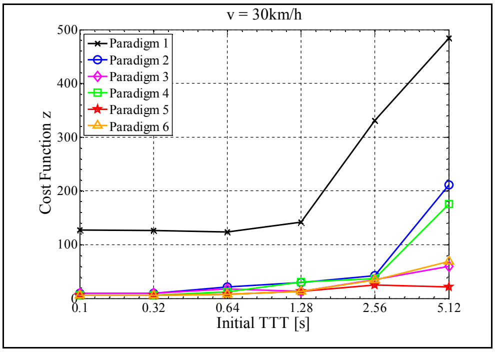

(d) Cost Function in 3G and LTE cells at 30km/h

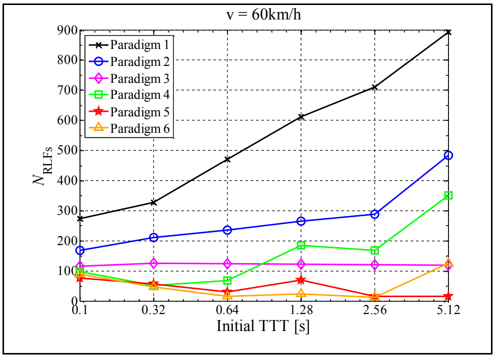

(e) Numbers of RLF in 3G and LTE cells at 60km/h

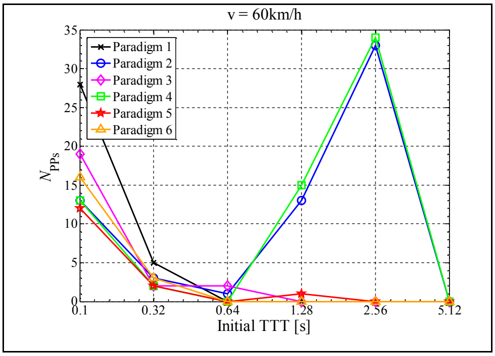

(f) Numbers of PP in 3G and LTE cells at 60km/h

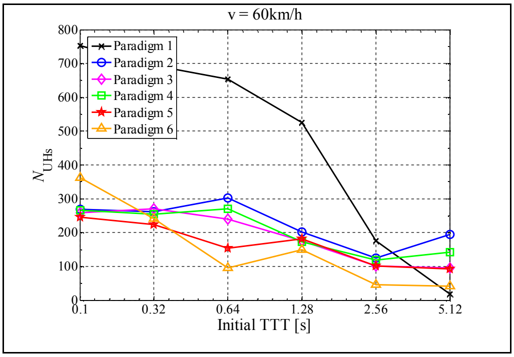

(g) Numbers of UH in 3G and LTE cells at 60km/h

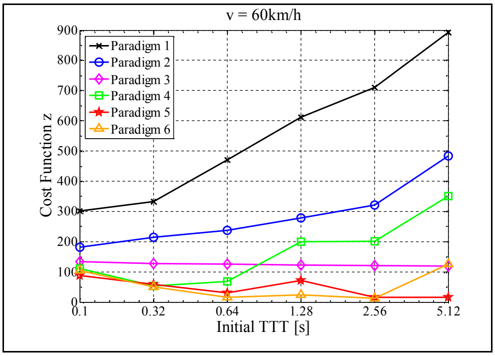

(h) Cost Function in 3G and LTE cells at 60km/h

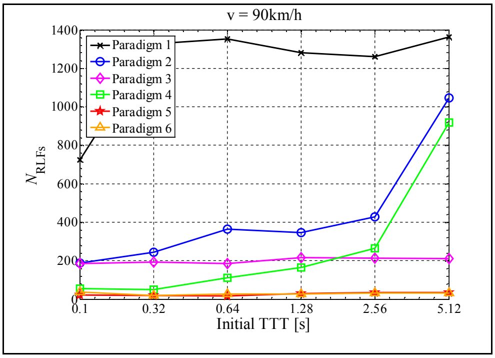

(i) Numbers of RLF in 3G and LTE cells at 90km/h

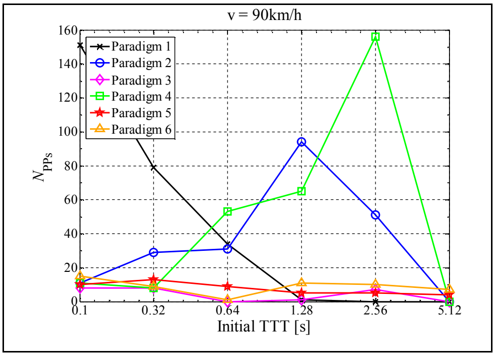

(j) Numbers of PP in 3G and LTE cells at 90km/h

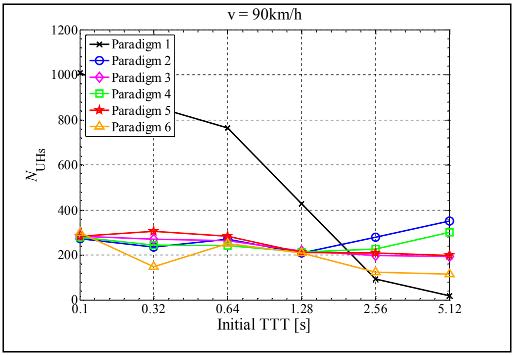

(k) Numbers of UH in 3G and LTE cells at 90km/h

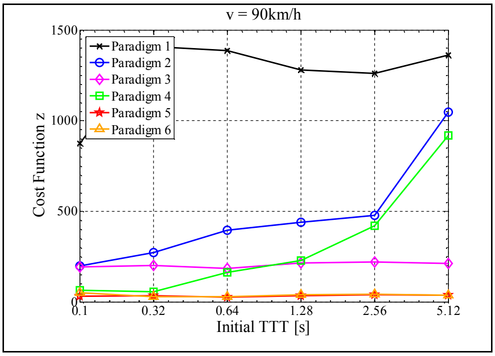

(l) Cost Function in 3G and LTE cells at 90km/h

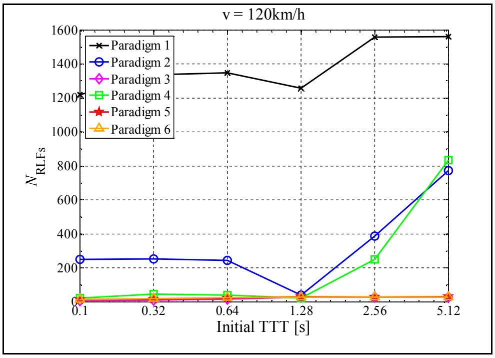

(m) Numbers of RLF in 3G and LTE cells at 120km/h

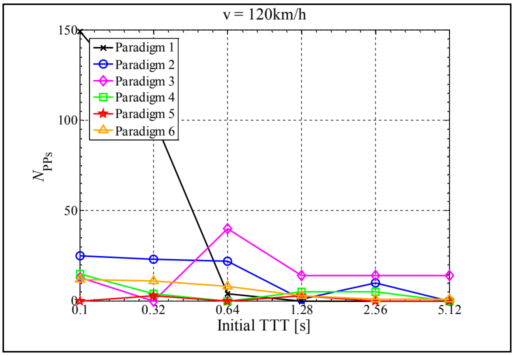

(n) Numbers of PP in 3G and LTE cells at 120km/h

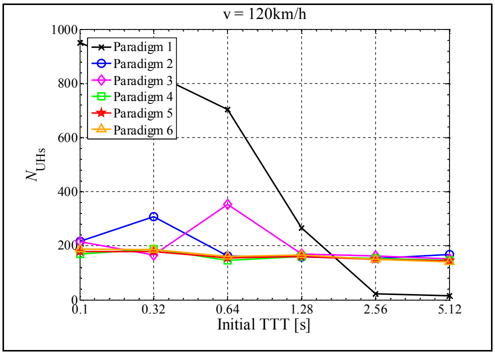

(o) Numbers of UH in 3G and LTE cells at 120km/h

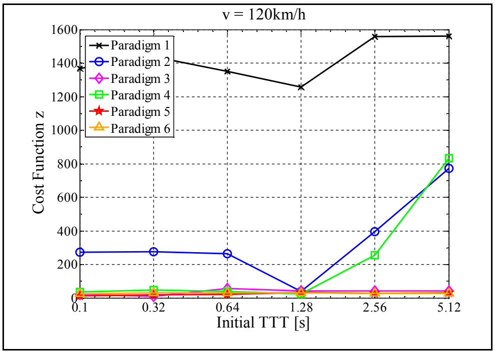

(p) Cost Function in 3G and LTE cells at 120km/h

Fig. 28 The performance of the six configuration paradigms with respect to the numbers of RLF, PP, UH and Cost Fucntion in 3G and LTE networks

The performance of cost function at higher speed 60km/h, 90km/h and 120km/h are similar with the one at 30km/h. According to Fig.28(h), Fig.28(l) and Fig.28(p) Paradigm 5 has lower mobility failure events than those achieved by other paradigms. Meanwhile, there is a significant decrease of the number of UHs even when RLF is reducing. In addition, Paradigm 5 achieves a flat curve performance on cost function which means regardless of different initial setting of TTT values the number of mobility failure events can be reduced to a certain low level. As we observe on Paradigm 2 and Paradigm 3 without coordinated TTT optimization in Fig.28(d), Fig.28(h) and Fig.28(i), the number of mobility failure events is the lowest at the smallest TTT value, e.g. $T_T = 0.1$s. That is, it's doubted to optimize the initial TTT value as initially it can be set to the smallest one. However, as the speed increased to 120km/h we discover that the best TTT is not always the smallest one. In Fig.28(p), without coordinated TTT optimization both Paradigm 2 and Paradigm 3 are able to reach the best performance at T_T=1.28s instead of T_T =0.1s. Therefore, a coordinated TTT and handover threshold optimization method is needed for this end and it is able to find the appropriate TTT values and handover thresholds autonomously and automatically without human intervention.

CHAPTER 6
Conclusions

This thesis work investigates a SON-based algorithm for optimizing the inter-RAT handover thresholds and TTT in a coordinated manner. The algorithm can be utilized in both 3G and LTE mobile systems. As TTT is one of the parameters that can trigger an inter-RAT measurement event, it can be used to optimize the handover performance by analyzing the handover procedure. The existing inter-RAT KPIs are maintained [10] but since TTT is involved as a parameter to be optimized the root cause is reanalyzed for each inter-RAT mobility failure event. Grouping KPI values to newly defined correction directives according to the action required by each mobility failure event to be applied on either handover thresholds or TTT. The coordination of the optimization of handover thresholds and TTT needs to sort out the same impact on specific KPIs. As a result, two new groups of slow handover and fast handover are defined in order to determine the executed parameter based on corresponding correction directives. As performance stability fails when TTT values oscillate, an oscillation detector for TTT is used to determine the type of parameter to be changed. Furthermore, a mapback controller is added to map back all mobility failure events which are grouped into TTT to the correction directives of handover thresholds.

The simulation results investigated at various speeds are shown that the coordinated optimization of inter-RAT handover thresholds and TTT outperforms the existing inter-RAT MRO algorithm [10] which only optimizes handover thresholds. Additionally, via the comparison among different optimization paradigms the jointly optimization of cell-pair-specific handover thresholds and cell-specific TTT obtains the largest gain from the default network-wide settings of handover thresholds and TTT. The performance results also show that to achieve the lowest cost function value the best TTT value is not always fixed to a certain value. This proofs the importance of applying an autonomous and automatic optimization algorithm to update the TTT value and handover thresholds.

CHAPTER 7
Future Work

The coordinated optimization algorithm will be extended to investigate in a new scenario which is close to real live networks. A potential scenario would be a typical irregular network layout for partly overlaying LTE network on top of 3G network. Most of the simulation parameters in new scenario are same with current scenario. The biggest difference is that the shadowing is modeled to be correlated for each radio link between two RATs according to 3GPP assumption [27]. However, the UEs are not able to be handed over from 3G to LTE because of the frequency band and path loss difference between two RATs. To this end, the traffic steering is used to guarantee the number of UE is in equilibrium between LTE and 3G networks. More study will be continued in the future.

References

[1] S.Hämäläinen, H.Sanneck and C.Sartori, *LTE Self-Organizing Networks (SON): Network Management Automation for Operational Efficiency*: John Wiley & Sons, 2011.

[2] 4GAmericas, "Self-Organizing Networks: The Benefits of SON in LTE," 2011.

[3] Z.Wei, "Mobility robustness optimization based on UE mobility for LTE system," in *Wireless Communications and Signal Processing (WCSP), 2010 International Conference on*, 2010, pp. 1-5.

[4] I.Viering, B.Wegmann, A.Lobinger, A.Awada and H.Martikainen, "Mobility robustness optimization beyond Doppler effect and WSS assumption," in *Wireless Communication Systems (ISWCS), 2011 8th International Symposium on*, 2011, pp. 186-191.

[5] T.Jansen, I.Balan, J.Turk, I.Moerman and T.Kurner, "Handover parameter optimization in LTE self-organizing networks," in *Vehicular Technology Conference Fall (VTC 2010-Fall), 2010 IEEE 72nd*, 2010, pp. 1-5.

[6] T.Jansen, I.Balan, S.Stefanski, I.Moerman and T.Kurner, "Weighted performance based handover parameter optimization in LTE," in *Vehicular Technology Conference (VTC Spring), 2011 IEEE 73rd*, 2011, pp. 1-5.

[7] I.Balan, T.Jansen, B.Sas, I.Moerman and T.Kurner, "Enhanced weighted performance based handover optimization in LTE," in *Future Network & Mobile Summit (FutureNetw), 2011*, 2011, pp. 1-8.

[8] A.Awada, B.Wegmann, D.Rose, I.Viering and A.Klein, "Towards self-organizing mobility robustness optimization in inter-RAT scenario," in *Vehicular Technology Conference (VTC Spring), 2011 IEEE 73rd*, 2011, pp. 1-5.

[9] A.Awada, B.Wegmann, I.Viering and A.Klein, "Self-Optimization Algorithm for Inter-RAT Configuration Parameters," in *Wireless Communication Systems (ISWCS), 2011 8th International Symposium on*, 2011, pp. 311-316.

[10] A.Awada, B.Wegmann, I.Viering and A.Klein, "A SON-based algorithm for the optimization of inter-RAT handover parameters," *submitted to IEEE Transactions on Vehicular Technology,* 2012.

[11] 3GPP, "Evolved Universal Terrestrial Radio Access Network (E-UTRAN); Self-configuring and self-optimizing network (SON) use

cases and solutions," in *TR 36.902*, ed. France: Sophia Antipolis, 2011.

[12] 3GPP, "Evolved Universal Terrestrial Radio Access (E-UTRA); radio resource control (RRC); protocol specification," in *TS 36.331*, ed. France: Sophia Antipolis, 2009.

[13] 3GPP, "Evolved universal terrestrial radio access (E-UTRA) and evolved universal terrestrial radio access network (E-UTRAN); overall description," in *TS 36.300*, ed. France: Sophia-Antipolis, 2011.

[14] J.Kurjenniemi and T.Henttonen, "Effect of Measurement Bandwidth to the Accuracy of Inter-frequency RSRP Measurements in LTE," in *Personal, Indoor and Mobile Radio Communications, 2008. PIMRC 2008. IEEE 19th International Symposium on*, 2008, pp. 1-5.

[15] 3GPP, "Evolved Universal Terrestrial Radio Access (E-UTRA); Physical layer; Measurements," in *TS 36.214*, ed. France: Sophia Antipolis, 2012.

[16] H.Holma and A.Toskala, *Lte for umts: evolution to lte-advanced*: Wiley, 2011.

[17] 3GPP, "Technical specification group radio access network; Physical layer; Measurements (FDD)," in *TS 25.215*, ed. France: Sophia Antipolis, 2011.

[18] 3GPP, "Evolved Universal Terrestrial Radio Access (E-UTRA); requirement for support of radio resource management," in *TS 36.133*, ed. France: Sophia Antipolis, 2010.

[19] UA.Bakshi and MV.Bakshi, *Modern control theory*: Technical Publications, 2009.

[20] 3GPP, "Performance Management (PM); Performance measurements Evolved Universal Terrestrial Radio Access Network (E-UTRAN)," in *TS 32.425*, ed. France: Sophia Antipolis, 2012.

[21] Y.Lee, B.Shin, J.Lim and D.Hong, "Effects of time-to-trigger parameter on handover performance in SON-based LTE systems," in *Communications (APCC), 2010 16th Asia-Pacific Conference on*, 2010, pp. 492-496.

[22] I.M.Balan, "Self organization in 3GPP long term evolution networks," 2012.

[23] A.Awada, B.Wegmann, I.Viering and A.Klein, "Cell-Pair Specific Optimization of the Inter-RAT Handover Parameters in SON," in *Proc. IEEE International Symposium on Personal, Indoor and Mobile radio communications*, 2012.

[24] A.F.Molisch, *Wireless Communications*: John Wiley & Sons, 2011.

[25] D.Aziz and R.Sigle, "Improvement of LTE handover performance through interference coordination," in *Vehicular Technology Conference, 2009. VTC Spring 2009. IEEE 69th*, 2009, pp. 1-5.
[26] M.Anas, F.D.Calabrese, P.E.Ostling, K.I.Pedersen and P.E.Mogensen, "Performance analysis of handover measurements and layer 3 filtering for UTRAN LTE," in *Personal, Indoor and Mobile Radio Communications, 2007. PIMRC 2007. IEEE 18th International Symposium on*, 2007, pp. 1-5.
[27] 3GPP, "Evolved Universal Terrestial Radio Access (E-UTRA); Further advancements for (E-UTRA) radio frequency system scenarios," in *TR 36.942*, ed. France: Sophia Antipolis, 2012.

List of Figures

List of Tables

List of Acronyms

2G	Second Generation
3G	Third Generation
3GPP	3rd Generation Partnership Project
CPICH	Primary Common Pilot Channel
CPS	Cell-Pair Specific
CS	Cell Specific
E-UTRA	Evolved Universal Terrestrial Radio Access
HWC	Handover to Wrong Cell
KPI	Key Performance Indicator
LTE	Long Term Evolution
MRO	Mobility Robustness Optimization
NW	Network-Wide
OFDM	Orthogonal Frequency-Division Multiplexing
OPEX	Operational Expense
PDCCH	Physical Downlink Control Channel
PDSCH	Physical Downlink Shared Channel
PP	Ping-Pong
PRB	Physical Resource Block
QoS	Quality of Experience
RACH	Random Access Channel
RAT	Radio Access Technology
RLF	Radio Link Failure
RNO	Radio Network Optimization
RSCP	Received Signal Code Power
RSRP	Reference Signal Receive Power
RSRQ	Reference Signal Receive Quality
RSSI	Received Signal Strength Indicator
SINR	Signal-to-Interference and Noise Ratio
SON	Self-Organizing Networks
TEH	Too Early Handover
TLH	Too Late Handover
TTT	Time-to-Trigger

UE	User Equipment
UH	Unnecessary Handover
UMTS	Universal Mobile Telecommunication System
UTRA	Terrestrial Radio Access

http://www.eit.lth.se